UNIVERSITY OF WITWATERSRAND, JOHANNESBURG

FACULTY OF HEALTH SCIENCES

SCHOOL OF PATHOLOGY

Functional consequences of novel IgG3 allelic variation CAP256-VRC26.25

Student Name: Fonguh Oliver Khan

Student Number: 2626981

Supervisor: Dr Simone Richardson (PhD)

Senior Medical Scientist (NICD) and Senior Researcher, University of the Witwatersrand

Co-supervisors: Professor Penny Moore (PhD)

Research Professor and Director: SA MRC Antibody Immunity Research Unit, University of the Witwatersrand and NICD

Dr Bronwen Lambson (PhD)

Senior Medical Scientist (NICD)

A Dissertation submitted to the Faculty of Health Sciences, University of the Witwatersrand, Johannesburg, in partial fulfilment of the requirements for the degree of Master of Science (Med) in Vaccinology.

Johannesburg, 2024

Declaration

I, Fonguh Oliver Khan, declare that this Research Report is my own unaided work. It is being submitted for the Degree of Master of Science (Medicine) in Vaccinology at the University of the Witwatersrand, Johannesburg. It has not been submitted before for any degree or examination at any other University.

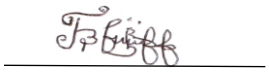

(Signature of candidate)

10th day of April 2024 in Parktown, Johannesburg, South Africa.

Abstract

Broadly neutralizing antibodies (bNAbs) isolated from HIV-1 individuals have shown promise in prevention. We have previously demonstrated that the IgG3 isotype significantly improved the neutralization potency of CAP256-VRC26.25 over the routinely used IgG1 constant region. However, there is significant allelic diversity in immunoglobulin constant heavy G chain 3 (*IGHG3*), especially in African populations, of which the functional relevance is unknown compared to IgG1 version. This study assessed whether allelic variation in IgG3 could further improve neutralization potency.

CAP256-VRC26.25 bNAb was engineered and expressed as 12 different IgG3 allelic variants, including two novel variants, as determined from previous *IGHG3* sequencing data from the CAPRISA 002 cohort. These were tested for neutralization against an eight-virus panel and compared to the IgG1 version.

Overall, the IgG3 versions of CAP256-VRC26.25 showed improved neutralization compared to the IgG1 version. Further, there were significant differences between allelic variants, IgG3*01 versus IgG3*04 (p=0.0038), IgG3*01 versus IgG3*15 (p=0.0013), IgG3*13 versus IgG3*04 (p=0.01570) and IgG3*13 versus IgG3*15 (p=0.0059). IgG3*01 showed the highest fold change (median value 8.0) relative to IgG1. IgG3*04 and IgG3*15 showed the least fold change (median value 2.2). This is due to the short hinge length of IgG3*04 and amino acid differences in IgG3*15. IgG3*01 and IgG3*13 were the most potent variants. This confirms the importance of the constant region in neutralization which has been supported by previous studies. Thus, hinge length and amino acid differences in the constant region impact neutralization.

This study shows that allelic variation in the constant region can impact on neutralization potency and supports leveraging genetic diversity to improve antibody function.

Acknowledgements

I would like to thank Wits for establishing the African Leadership in Vaccinology expertise (ALIVE) Flagship research entity and to Dr Clare Cutland and Kay Roberts for the Coordination and organization of the training. I also thank the Board members of ALIVE.

I would also like thank the Bill and Melinda Gates Foundation, and other partners for providing the funds which enable me to carry out my studies smoothly.

I would like to express my profound gratitude to my supervisors Dr Simone Richardson, Professor Penny Moore and Dr Bronwen Lambson for the technical skills and enormous moral support they gave in carrying out and writing my research report.

I thank all the members of staff of the Antibody Immunity Research Unit (AIRU), National Institute for Communicable Diseases (NICD) of the National Laboratory Health Service for training me in all laboratory techniques: Donald Mhlanga, Strauss van Graan, Sinethemba Bhebhe, Tandile Modise, Qiniso Mkhize, Thamara Naidoo and acknowledge the NIH U01 grant under H3 Africa for funding the research contained in this project.

I thank my wife, children and family at home who endured my absence during my study period and the continuous encouragement they gave. To my family and friends in Johannesburg, for the support and care.

I thank my classmates for the collaboration we had during our training, always working together as a team to succeed and to other friends who encouraged me in one way or the other.

Table of Contents

List of Figures

List of Tables

List of Abbreviations

ADCC: Antibody-dependent cellular cytotoxicity

ADCD: Antibody-dependent complement deposition

ADCP: Antibody-dependent cellular phagocytosis

AID: Activation-induced cytidine deaminase

AMP: Antibody mediated prevention

ART: Antiretroviral Therapy

BCR: B cell receptor

bNAb: Broadly neutralizing antibodies

CAPRISA: Centre for the AIDS programme of research in South Africa

CDbs: CD4 binding site

CDC: Complement dependent cytotoxicity

CDR H3: Complementarity-determining region H3 loop

CSR: Class switch recombination

DNA: Deoxyribonucleic acid

DMC: Data monitoring committee

DMEM: Dulbecco`s Modified Eagle Medium

Fab: Fragment antigen binding

Fc: Fragment crystallizable

FcɣR: Fc gamma receptor

GMT: Geometric mean titre

ART: Antiretroviral Therapy

HEK: Human embryonic kidney

HIV: Human Immunodeficiency Virus

HPTN: HIV prevention trial network

HVTN: HIV vaccine trail network

IGHG: Immunoglobulin constant heavy G chain

IMGT®: the international ImMunoGeneTics information system®

ITAM: Immunoreceptor tyrosine-based activation motif

ITIM: Immunoreceptor tyrosine-based inhibition motif

LB: Luria-Bertani

MAC: Membrane attack complex

MPER: Membrane proximal external region

NK: Natural killer cells

PBMC: Peripheral blood mononuclear cells

PCR: Polymerase chain reaction

PEI: Polyethylenimine

RLU: Relative light units

UNAIDS: The Joint United Nations Program on HIV/AIDS

1.0 Introduction

1.1 The Global burden of HIV

Human Immunodeficiency Virus (HIV) has been a major global public health concern since its discovery in 1981(1). One of the main challenges has been the development of vaccines to prevent transmission to uninfected individuals (2,3). However, antiretroviral therapy (ART) has contributed significantly to decreasing viral load and limiting the advancement of disease and HIV spread (4). According to UNAIDS global HIV estimates, 39 million people were living with HIV, among which are 1.3 million new infections in 2022 (5). This illustrates the urgent need for an effective, safe, and cost effective vaccine that is accessible with ease globally (6). Specifically in South Africa, 7.5 million people are currently living with HIV and two million of these individuals remain virally unsuppressed and are ART naïve (7).

1.2 The elusive goal of the HIV vaccine

There are several challenges associated with vaccine development against HIV. HIV mutates at a high rate, largely driven by reverse transcriptase that is prone to errors and recombination during replication (8). This has contributed significantly to the viral envelope (Env) glycoprotein genetic diversity which is the major target of neutralizing antibodies (9). In order to protect from infection, an HIV vaccine that elicits broadly cross-reactive immune responses capable of neutralizing diverse viruses is required. The HIV Env bears extensive host N-linked glycosylation that effectively shields many conserved epitopes on the trimer from antibody recognition (10,11). Other challenges include inadequate knowledge of the correlates of immune protection and unavailability of an inexpensive animal model (12,13).

There have been over 250 HIV vaccine trials with most of them ending at phase 1 or 2 (early-phases) (14). Early HIV vaccine concepts were focused on humoral anti-HIV immune responses to induce neutralizing antibodies (NAbs) targeting monomeric HIV-1 Env gp120 (15). This paved the way for subsequent studies with the goal to elicit both cellular immune and humoral responses including VaxSyn (16), HIVAC-1e (17) and vCP125, an ALVAC-HIV vector, a gp160 expressing vaccine, VAX003 and VAX004 (18,19) and HVTN 505 a tetravalent adenovirus vector vaccine (20). All these trials were terminated due to lack of efficacy. The first vaccine to show any efficacy was the RV144 vaccine, a recombinant canarypox vector vaccine [ALVAC-HIV (vCP1521)] boosted with

two shots of a recombinant gp120 subunit (AIDSVAX B/E) and administered to 16,402 healthy men and women in Thailand. This showed an efficacy of 31.2% which was modest but significant in reducing HIV-1 infection rate (21). In the RV144 trial, Fc effector functions but not neutralization correlated with decreased infection rate (22–24), specifically those targeting the V1/V2 Env region (25,26). This prompted many follow-up trials that aimed to elicit potent Fc effector functions including HVTN 097 using the same immunogens as RV144 in a South African population (27) and HVTN 100 making use of a subtype C gp120 insert (28). These prompted the HVTN 702 phase 2b/3 efficacy study using the immunogens from HVTN 100. However, the study was discontinued following interim data review by the data monitoring committee (DMC) for lack of efficacy in preventing HIV infection in vaccine recipients (29).

While vaccine strategies have not yet been effective, it is still widely accepted that a vaccine must induce broadly neutralizing antibodies. This remains a challenge owing to the length of time required to develop them in natural infection and the complex mechanisms involved with viral co-evolution, complicating the identification of the initiating immunogen. A crucial step in their induction is the stimulation of naïve B cells capable of developing bNAbs, which currently is a major research focus in the vaccine field (30). These subsets of B cells are usually few in the human naïve B cell repertoire and have low or no affinity for current HIV vaccine immunogens (31).

While vaccines are not yet successful in inducing bNAbs, passive immunization with these neutralizing antibodies has proven to be promising. The HVTN 703/HPTN 085 and HVTN 703/HTPN 081 trials or the antibody mediated prevention (AMP) study assessed the efficacy, tolerability, and safety of VRC01, a CD4 binding site bNAb on the HIV-1 Env glycoprotein to prevent HIV infection (32). VRC01 recipients acquired only viral strains that were very resistant to VRC01 compared to strains that infected participants who received placebo. This shows that protection was conferred only against VRC01 sensitive viruses but not overall prevention of HIV-1 infection. However, this showed proof of concept that bNAbs can be administered as prophylaxis (32).

1.3 Structure of the Human Immunodeficiency Virus envelope

HIV-1 is a positive sense-RNA enveloped virus having a 9.8kb RNA genome that codes for three polyproteins (Env, Gag, and Pol) including other accessory proteins like Vpr, Vpu, Tat, Vif, Nef and Rev (33). The envelope glycoprotein (Env) is essential for viral

attachment and penetration into cells expressing the CD4 receptor and CCR5 or CXCR4 co-receptor mainly on helper T lymphocytes (34).

The HIV Env is made up of gp160 trimer precursor polypeptide, which cleaves to form the gp120 surface unit and the gp41 transmembrane unit that are noncovalently bound. The surface glycoprotein (gp120) trimer is comprised of five variable regions (V1-V5) and five constant regions (C1-C5), and the transmembrane glycoprotein (gp41) trimer comprised of the fusion peptide, the heptad repeat domains (HR1 and HR2) and the membrane proximal external region (MPER). N-linked glycans from the host are added to the Env during the early stages of protein synthesis at the level of the endoplasmic reticulum prior to leaving the Golgi apparatus (35).

The gp160 Env trimer facilitates viral binding to $CD4^+$ on the surface of the cell followed by conformational changes leading to binding with CCR5 or CXCR4 co-receptor and fusion of gp41 Env trimer to the membrane of the cell (36). The main target for humoral responses is the HIV-1 Env trimer which can either be presented as the pre-fusion "closed" conformation recognized by bNAbs (37–40) or the "opened" CD4-bound conformation mainly recognized by non-neutralizing antibodies (39,41–43).

1.4.0 Antibodies

1.4.1 The Structure of an Antibody

An antibody has a Y-shaped structure that is comprised of four polypeptide chains (two heavy chains and two light chains). These polypeptide chains are linked up to form three structural domains composed of two antigen binding fragments (Fab), one fragment crystallizable (Fc) and a flexible hinge region that proteases can easily digest to form the Fab and Fc portions. The Fc portion consist of the heavy constant 2 (CH2) and heavy constant 3 (CH3) domains while the Fab portion is comprised of both variable light (VL) region and constant light (CL) region linked to the variable heavy (VH) region and constant heavy 1 (CH1) domain (Figure 1.2) (44). The heavy chain and the light chain are linked together by disulfide bonds (Figure 1.2). The hinge region is a short sequence separating CH1 and CH2 linking the Fab and Fc fragments of the antibody. The hinge region in conjunction with CH2 and CH3 Fc region allow for dimerization of the heavy chain polypeptides. The length of the hinge region confers some stability and flexibility in the antibody and impacts on its Fab and Fc effector functions (45,46). Although the isotypes

and subclasses (defined by the constant region) have different amino acid sequences, as suggested by its name, the constant region (CH1-3) folds into a similar structure consisting of beta-pleated sheets held together by intrachain disulfide bonds (figure 1.1) (47).

While the Fab fragment confers antigenic specificity, the Fc fragment defines the effector functions of the antibody. The Fab fragment binds to the antigen and neutralizes the pathogen or blocks it from infecting other cells. The Fc fragment mediates Fc effector functions by binding to Fc gamma receptors (FcγR) on effector cells or binding complement proteins (48). The Fc region also influences the antibody binding affinity, thus affecting antigen recognition and neutralization (49).

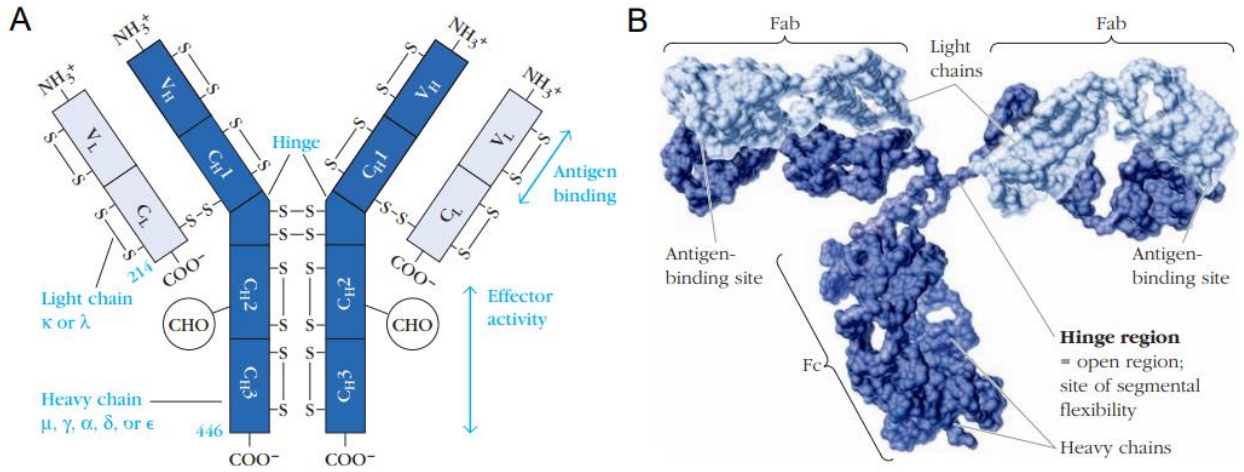

Figure 1.1: Structure of an antibody. (A) the heavy chain is shown in blue with the variable heavy region (VH), constant heavy domains (CH 1-3), the light chain shown in light blue is comprised of the variable light region (VL) and the constant light domain (CL), the hinge region link up the heavy and the light chains with disulphide (S=S) bonds, (B) shows the antigen-binding site (Fab) of both the heavy and light chains, the hinge region and the Fc portion of the heavy chain. Figure adopted from Creative Biolabs) *(47)*

1.4.2 Antibody functions in response to HIV infection

1.4.2.1 HIV-1 neutralizing antibody (NAb) target sites and broadly neutralizing antibodies

Neutralization occurs when the Fab region of an antibody binds to a pathogen, blocking it from infecting cells. Most HIV neutralizing antibodies developed during natural infection are strain-specific for the circulating viruses in the body (50). However, a subset of HIV-infected individuals (10-30%) develop bNAbs after one to three years of infection and many of these bNAbs have been cloned and characterized (51–53). These antibodies recognize epitopes on gp120 and gp41, as well as quaternary epitopes. Seven bNAb target sites have been identified on the envelope glycoprotein of HIV-1 (Figure 1.2) namely: the fusion peptide (targeted by PGT151, VRC34), silent face (targeted by VRC-PG05), V2/apex (PG9/PG16, CAP256-VRC26.25, PGT145), MPER (2F5, 4E10), gp120/gp41 (PGT151-PGT158), CD4 binding site (CD4bs) (VRC01-VRC03/NIH45-46, 8ANC131) and the N332-supersite (PGT 121-PGT 123/10-1074) (54,55).

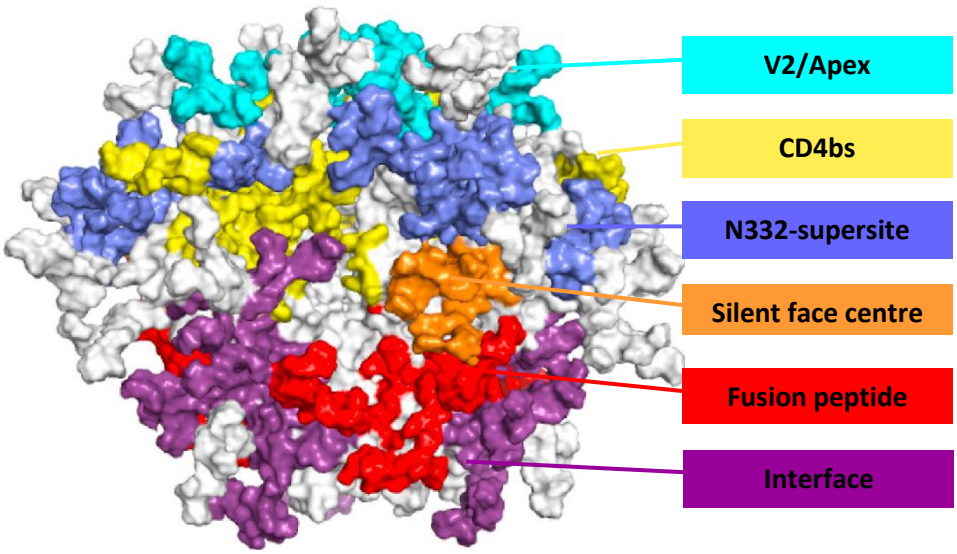

Figure 1.2: The structure of HIV-1 prefusion-closed Env trimer showing epitopes of six categories of bNAbs. The different colours represent the V2/Apex (cyan), CD4 binding site (yellow), N332-super (blue), silent face (orange), fusion peptide (red), and interface (purple). MPER is not indicated on the diagram since it is not present on the BG505.664 SOSIP trimer shown here. Figure adopted from Kwong and Mascola (2018) *(56)*.

1.4.3 Fc effector functions and Fc receptors

In addition to neutralization, antibodies can bind to Fc receptors or complement proteins to elicit cytotoxic function. Fc effector functions can clear infected cells or viruses in several ways, which include antibody-dependent cellular phagocytosis (ADCP), antibody-dependent cellular cytotoxicity (ADCC), and complement-dependent cytotoxicity (CDC) (57).

Following ADCC, Natural killer (NK) cells are attracted through binding of the Fc portion of antibodies to the Fc-gamma receptor IIIa (FcγRIIIa) followed by secretion of perforins and granzymes thereby lysing the cell (Figure 1.3) (58). In the RV144 vaccine clinical trial, ADCC was observed to be associated with protection (21,59)**.** ADCP occurs when FcγRIa and FcγRIIa on the surface of monocytes, macrophages, or neutrophils bind to the Fc portion of an antibody to an antigen-antibody complex engulfing viruses or infected cells and destroying them with lytic enzymes found in the endosome (Figure 1.3) (58). Finally, complement deposition involves C1q bound to the Fc domain along with other proteins form pores on the surface of the infected cell or virus known as membrane attack complex (MAC) that punctures the cell resulting in lysis (58).

These Fc effector functions have been observed to play a protective role in vaccines and are also necessary for maximum protection afforded by bNAbs (21,60–62). The Fc-dependent function is necessary for bNAbs to completely protect from infection, suppress viral load and/or clear infected cells (61). Different mechanisms including Fc receptor binding affinity and antibody isotype modulate Fc effector functions.

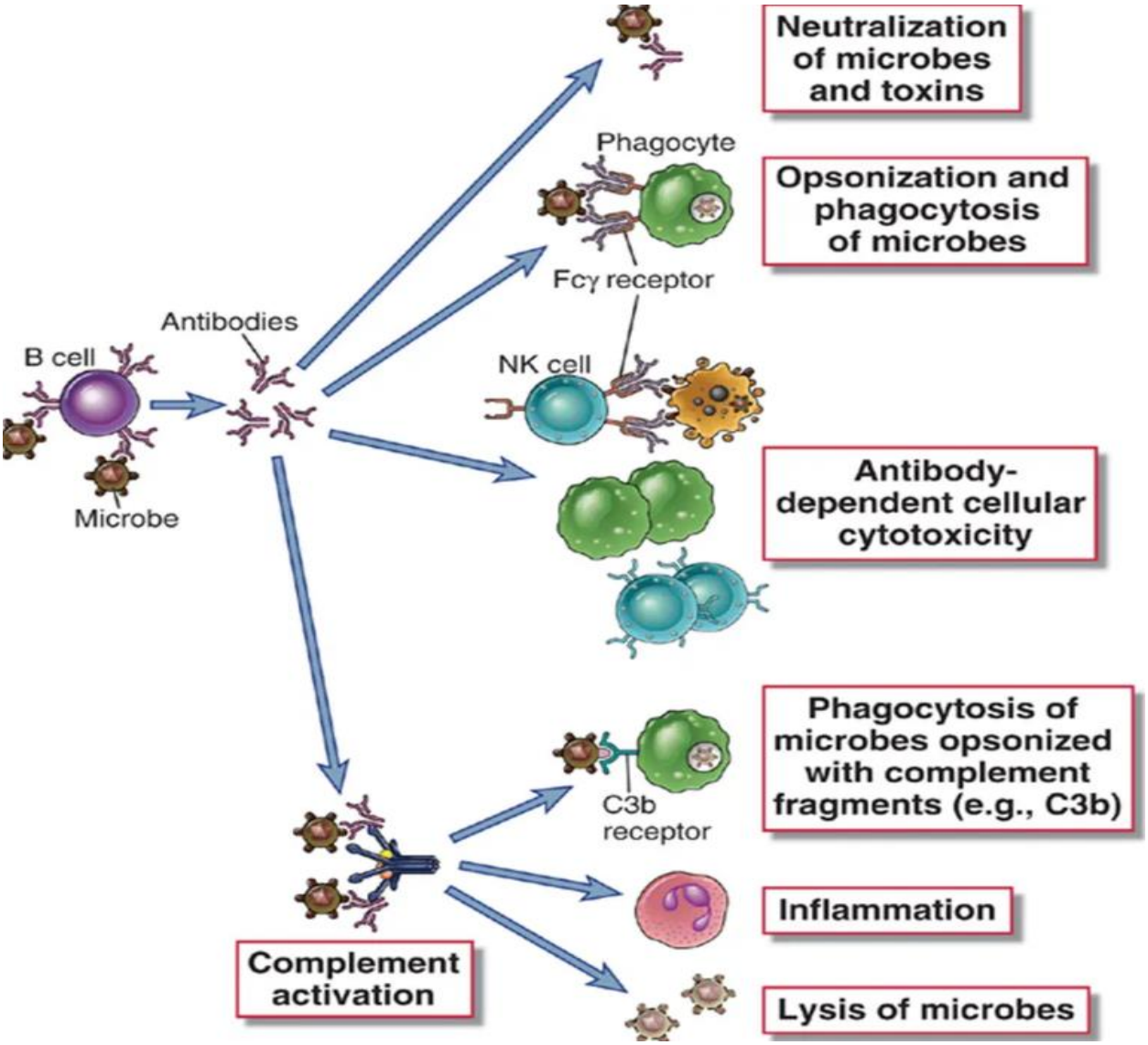

Figure 1.3: Antibody functions. Neutralization: The Fab region of an antibody bound to its cognate epitope, blocking viruses from infecting cells. Fc effector functions: The FcγR on the cytoplasmic membrane of natural killer (NK) cells binds to the Fc domain of an antibody of an infected cell causing cytotoxicity. Complement proteins deposited on the Fc domain of an antibody-antigen complex enhancing phagocytosis**.** Complement proteins deposited on the envelope glycoprotein of viruses form pores on the membrane resulting in lysis. Figure adopted from Saunders (2011) *(58)*.

1.4.4 Fc receptors

The cells of the innate immune system such as NK cells, neutrophils, monocytes, and macrophages, express membrane receptors capable of binding to the Fc portion of antibodies (FcR). These receptors perform different biological functions modulated by aggregation of multivalent formation of antigen-antibody complexes (63). FcR receptors

are classified as activating if they have immunoreceptor tyrosine-based activation motifs (ITAMs) (64) in the intracytoplasmic domain or inhibitory if they possess an immunoreceptor inhibitory motif (ITIM) in the intracytoplasmic domain. They are comprised of low and high-affinity receptors (65). Low-affinity and High-affinity FcɣR are distinguished by how they bind to IgG during immune complex formation with a firm avidity. However, only high-affinity FcɣR can bind the monomeric IgG (66). Human hFcɣRI (CD64) is the only IgG high-affinity FcɣR in humans while FcɣRIIa, IIb and IIc (CD32) are two families of low-affinity IgG receptors, including FcɣRIIIa and IIIb (CD16). FcɣR-associated activating receptors are comprised of FcɣRIIa and FcɣRIIc. The single-chain inhibitory receptors are the FcɣRIIb (63) and FcɣRIIIb constitute the glycosylphosphatidylinositol (GPI)-linked receptors that induce calcium entry *via* transient receptor potential melastatin 2 in neutrophils (67).

1.5 Antibody Isotypes

The heavy constant chain (*IGHC*) genes define an antibody isotype. Depending on the heavy chain they possess, five classes of immunoglobulins isotypes have been defined comprised of IgM, IgD, IgE, IgG (IgG 1-4), and IgA (IgA 1-2) (Figure 1.4). IgM is a monomer anchored on the surface of B cells as a B cell receptor (BCR) while the secretory form (sIgM) is a pentamer. IgM is produced when it encounters an antigen by short-lived plasma cells extrafollicularly or long-lived affinity-matured plasma cells (68). IgM is a suitable activator of complement and neutralization. IgA is a monomer when bound to mucosal membranes. Most circulating IgA in serum exists as a monomer while the IgA found on mucosal surfaces is dimeric (69). IgE is a monomer associated with hypersensitivity and allergic reactions as well as against infections with parasites. IgD is a membrane-bound antibody together with IgM on the surface of B cells. Serum levels of IgD are deficient with a very short half-life. IgG is the most predominant isotype in the body. It has the longest half-life of all the different isotypes and is the most extensively studied immunoglobulin. Isotype alters the half-life of an antibody (70), antigen-binding valency (71) or FcɣRs binding affinity (72). Immunoglobulins are converted from one isotype to another through class switching.

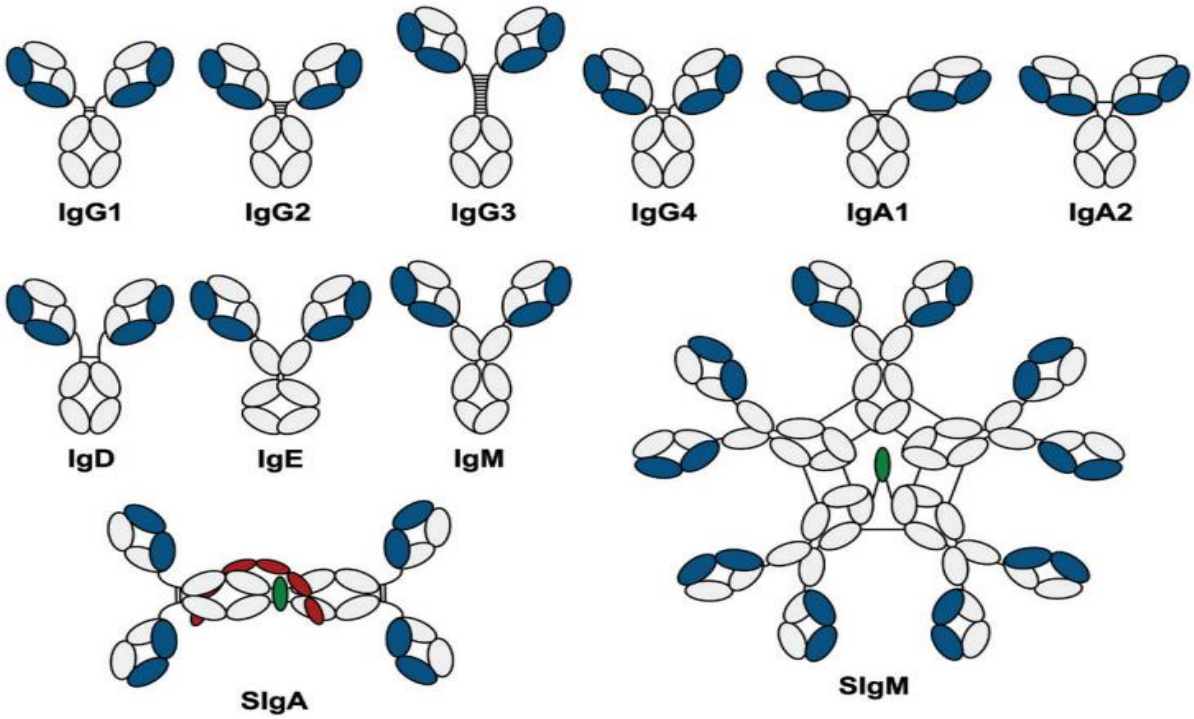

Figure 1.4: Antibody isotypes**:** The five classes are comprised of IgM, IgD, IgG, IgE and IgA and subclasses (IgG1-4 and IgA1-2). Antibody isotypes differ by Fc regions consisting of two similar heavy (white) and light (blue) chains and an N-terminal variable region and a C-terminal constant domain. The secretory IgM (SIgM) exists as a pentamer while secretory IgA (SIgA) is a dimer, IgG, IgD and IgE are monomers. IgG encompasses IgG1, IgG2, IgG3 and IgG4. IgG3 has a long hinge length than any other IgG subclasses while IgA is comprised of IgA1 and IgA2 *(73)*.

1.6 Class Switch Recombination

Antibodies can switch from one isotype to another dependent on the cytokines elicited in response to infection by the process of class switch recombination (CSR) enhanced by the enzyme Activation-induced cytidine deaminase (AID) (74). During CSR, the switch (S) region located upstream of each constant region gene (except for Cδ) is targeted by AID. Induction of AID is elicited jointly by interleukin-4 (IL-4) and CD40 signaling, which removes an amino group on cytosines in donor and acceptor S regions to form uracils. Thus, mismatched repair mechanisms lead to the introduction of single-stranded DNA (ssDNA) breaks and non-homologous end repair (Figure 1.5).

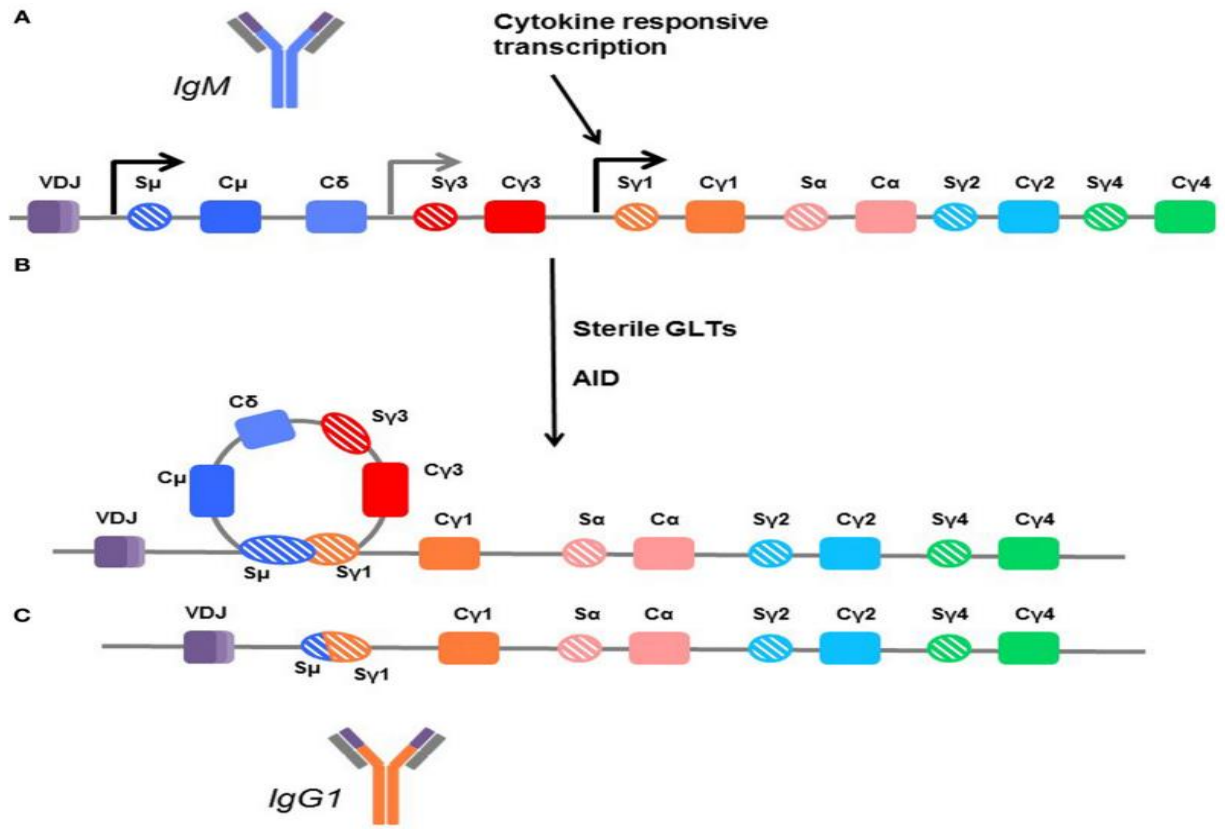

Figure 1.5: Class switch recombination (CSR) with *IGHG* gene in a naive B cell expressing both IgM and IgD. AID introduces permanent deletions on the switch-region to remove Cμ and Cδ genes. Antibody is secreted as a different isotype with the same V-region *(74)*.

1.7 Immunoglobulin G (IgG) and genetic determinants of isotype

IgG is one of the most abundant antibodies in plasma, accounting for about 10-20% of plasma proteins. IgG is comprised of IgG1, IgG2, IgG3 and IgG4 subclasses encoded by distinct Ig heavy constant chain (*IGHC*) genetic loci, *IGHG1*, *IGHG2*, *IGHG3* and *IGHG4* (75). Each subclass has a unique profile regarding binding to antigens, complement activation, immune complex formation, antibody half-life and mediation of Fc effector functions (76) (Table 1.1). IgG subclasses perform different responses whereby IgG1 and IgG3 elicit pro-inflammatory responses whereas IgG2 and IgG4 induce anti-inflammatory responses and/or immune tolerance (73). The IgG genes span a ~150 kb region within the *IGHG* locus on human chromosome 14. IgG domains are comprised of CH1, hinge, CH2 and CH3 encoded by separate exons. Genetic polymorphism within each subclass has been studied and there are multiple alleles registered in the international ImMunoGeneTics (IMGT) database (77).

There are 14 alleles in *IGHG1* that encode 6 different antibody versions (78). The functional consequences of these *IGHG* polymorphisms are incompletely understood (77). Variations between these antibodies include single nucleotide polymorphisms (SNPs) or differences in hinge lengths.

Table 1. 1 The structure and polyfunctionality of IgG subclasses: The structure of each isotype is represented above the column. The relative strength of each function is indicated by the number of "positive", and the absence of the function as "negative " *(79)*.

Function	IgG1	IgG2	IgG3	IgG4
Phagocytosis	++	-	+++	+
ADCC	++	-	+++	-
Complement	++	+	++	-
Neutralization	++	++	++	++

1.8.1 Immunoglobulin G3 (IgG3)

IgG3 appears very rapidly following HIV infections (80) and it is the most polyfunctional subclass of IgG eliciting a potent complement activation and binds FcγRs with high affinity to drive Fc effector functions (45,46) (Table 1.1). IgG3 has the longest hinge region which confers a high degree of flexibility involved in antiviral activity (45). It has been noted that the concentration of IgG3 tends to reduce as infection persists or progresses in the body (81). There are 29 *IGHG3* reported alleles registered in IMGT (82) but the functions of these alleles have not been fully studied.

1.8.2 Using IgG3 to improve the function of bnAbs

Previous studies from our laboratory have shown that IgG3 significantly enhances both ADCP and neutralization of a potent bNAb, CAP256-VRC26.25 (45). Further, this was mediated by the length of the hinge region (45). In other bNAbs such as VRC01, the

increased hinge length compared to IgG1 was directly related to increased phagocytic activity (46). Another study of a panel of 15 bNAbs targeting several epitopes and expressed as IgG1 and IgG3 versions showed IgG3 bNAbs in general demonstrated the same or enhanced (up to 60-fold) neutralization potency than IgG1 versions, although this effect was specific for each virus (83). This enhanced potency was especially prominent for CAP256-VRC26.25, CAP255.G3, PGT135 and 35022. Improved ADCP was observed in all IgG3 bNAbs over IgG1 versions. In ADCC, differences were epitope specific, with IgG3 bNAbs to the CD4 binding site, MPER and gp120-gp41 interface showing enhanced ADCC. Although IgG3 bNAbs have neutralization potency and enhance Fc effector functions, they are not used clinically due to their short half-life of approximately seven days compared to IgG1 of 21 days. However, there are several allelic variants of IgG3 with half-lives similar to IgG1 (70), and further, we have shown that IgG3 bNAbs engineered using the lambda light chains have the same pH dependence on the neonatal Fc receptor (FcRn) to their IgG1 counterparts, suggesting similar half-life (83). This demonstrates that challenges of the IgG3 short half-life can be overcome and IgG3 used clinically as a novel mechanism to enhance neutralization potency and Fc effector functions of HIV bNAbs.

1.8.3 Allelic variation in the IgG3 constant region impacts antibody function

The IgG heavy chain is very polymorphic (IgG allotypes) introducing a second level of variation. These IgG allotypes were initially identified serologically by hemagglutination inhibition tests (84). Immunoglobulin gene sequencing from diverse ethnic groups has shown more allelic versions that were not detected by serological methods, especially in IgG3 (84,85). Current advancements in genetic sequencing techniques have paved the way for identifying IgG3 allelic variants. There are 29 IgG3 alleles identified and annotated in IMGT (78) with differences based on single nucleotide polymorphisms (SNPs) or differences in hinge lengths in *IGHG3*. Studies have shown that changes can greatly influence both antibody assembly and stability in the amino acid sequence (86). Replacing asparagine at position 392 on the CH3 domain of *IGHG3*03* with lysine weakens CH3-CH3 interaction, which dissociates significantly faster than IgG4 (87). A study conducted systematically on 27 unique IgG alleles on Fc receptor binding revealed that amino acid sequence differences in IgG3 versions were the major driver in the alteration of Fc receptor binding (88). The observed differences were attributed individually to the number of hinges and the presence of specific amino acid changes in

the CH2 region at positions 291, 292, and 296 (87). Studies have shown that variations in the naturally occurring heavy chain amino acids are promising for passive immunization strategies, with several alleles having an extended half-life for example (70) .

Human immunodeficiency virus (HIV) is a virus from the Retrovirus family that attacks human immune cells, especially T lymphocytes. The increasing number of HIV cases requires a more effective preventive measure, among others, through vaccination. Although it has been over 40 years, there is no HIV vaccine yet. This is attributed to variations in HIV Env or genetic material, and each country has its own dominant HIV variant. In addition, the ability of HIV to evade immune responses, high mutation rates, and limited experimental animals add to the difficulties in developing effective vaccines. As of May 2022, 16 vaccines have undergone phase I/II clinical trials. Among HIV vaccines that have already undergone phase III clinical trials, only RV 144 vaccine gave promising results, with efficacy reaching 31.2%. The development of the HIV vaccine continues to obtain a safe and effective HIV vaccine. Some of these allelic variants have been studied and shown enhanced neutralization potency and Fc effector functions (45,83). However, some of these alleles have not yet been systematically studied. This project aimed to assess the functional consequences of IgG3 allelic variants on CAP256-VRC26.25 isolated from an HIV infection individual.

1.9 CAP256-VRC26.25: A bNAb with increased potency as an IgG3 class switch variant

CAP256-VRC26.25 is part of a broadly neutralizing antibody lineage isolated from an HIV-infected individual CAP256 who was enrolled in the CAPRISA 002 Acute Infection Study (89). The constant region of bNAb lineage members from CAP256 was sequenced and found to use a novel IgG3 allele *IGHG3*01m*. This antibody was isolated from B cells in cultured peripheral blood mononuclear cells (PBMCs) collected at 193 weeks, corresponding to the peak period of antibody neutralization breadth and potency (90). CAP256-VRC26.25 belongs to the V2-glycan apex epitope-targeting bNAbs which are very potent group of antibodies with a geometric mean titer (GMT) of about 0.3 µg/mL and a breadth of 71% against the global HIV-1 viruses (91). CAP256-VRC26.25 has a long protruding tyrosine-sulfated, anionic CDR H3 loop comprised of 36 amino acids, critical to its mode of recognition (92). CAP256-VRC26.25 is presently being studied in a clinical trial (PACTR202003767867253) to assess its ability to prevent HIV infection in combination with other bNAbs (93,94).

In previous studies, CAP256-VRC26.25 expressed as IgG3 subclass showed both enhanced neutralization and Fc effector functions, with different functions detected between the two IgG3 alleles the individual used, IgG3*17 and IgG3*01m (45). This study highlights the value of allelic variation to improve the function of bNAbs. A previous study sequenced the *IGHG3* genes of 10 HIV-infected individuals from the CAPRISA 002 infection cohort and found the population to express variable alleles. Using Sanger and PacBio platforms, five novel *IGHG3* alleles were identified, three of which contained amino acid substitutions in coding regions. A further ten documented alleles were identified from nine participants. Studying different *IGHG3* allelic forms of CAP256-VRC26.25 identified in African individuals is likely to contribute to the understanding of the improvement of this bNAb for HIV prevention and therapy.

1.10 Aims and Objectives

The overall aim of this project was to determine the effects of different IgG3 allelic variants and specific mutations within those alleles on antibody function.

1.10.1 Specific objectives

Objective 1: To engineer novel IgG3 allelic variants of bNAb CAP256-VRC26.25.

Objective 2: To compare the neutralization functions of CAP256-VRC26.25 allelic variants.

2.0 Materials and Methods

2.1 Ethics Approval

This study was approved by the Human Research Ethics Committee of the University of the Witwatersrand (Medical) for which it issued a waiver (M2211125) as a sub-study under the parent project ethics approval (M210892).

2.3.0 Antibody design and production

A broadly neutralizing antibody CAP256-VRC26.25 isolated from an HIV-positive South African woman enrolled in the CAPRISA 002 Acute infection cohort (95) was used for this project. Twelve IgG3 allelic variants (*IGHG3*01*, *IGHG3*01m*, *IGHG3*03*, *IGHG3*04*, *IGHG3*11*, *IGHG3*11mm*, *IGHG3*12*, *IGHG3*13*, *IGHG3*14*, *IGHG3*15*, *IGHG3*16*, and *IGHG3*17*) (Figure 2.1) of CAP256-VRC26.25 were engineered. These alleles were previously found in other African individuals from the CAPRISA 002 cohort (96). CAP256.VRC26.25 allelic variant expression plasmids for IgG3*01, IgG3*01m, IgG3*04, IgG3*11mm, IgG3*12 and IgG3*14 were already available while IgG1 and IgG3*17 were already expressed. The amino acid sequences of IgG3*15 and IgG3*16 differ from IgG3*14 by one amino acid change in the CH3 and CH2 regions of the heavy chain respectively, the plasmid for IgG3*14 readily available in our lab was used to produce IgG3*15 and IgG3*16. Mutations were introduced into the constant region of IgG3*14 to make IgG3*15 (CH3 N392K) and IgG3*16 (CH2 T339A) alleles.

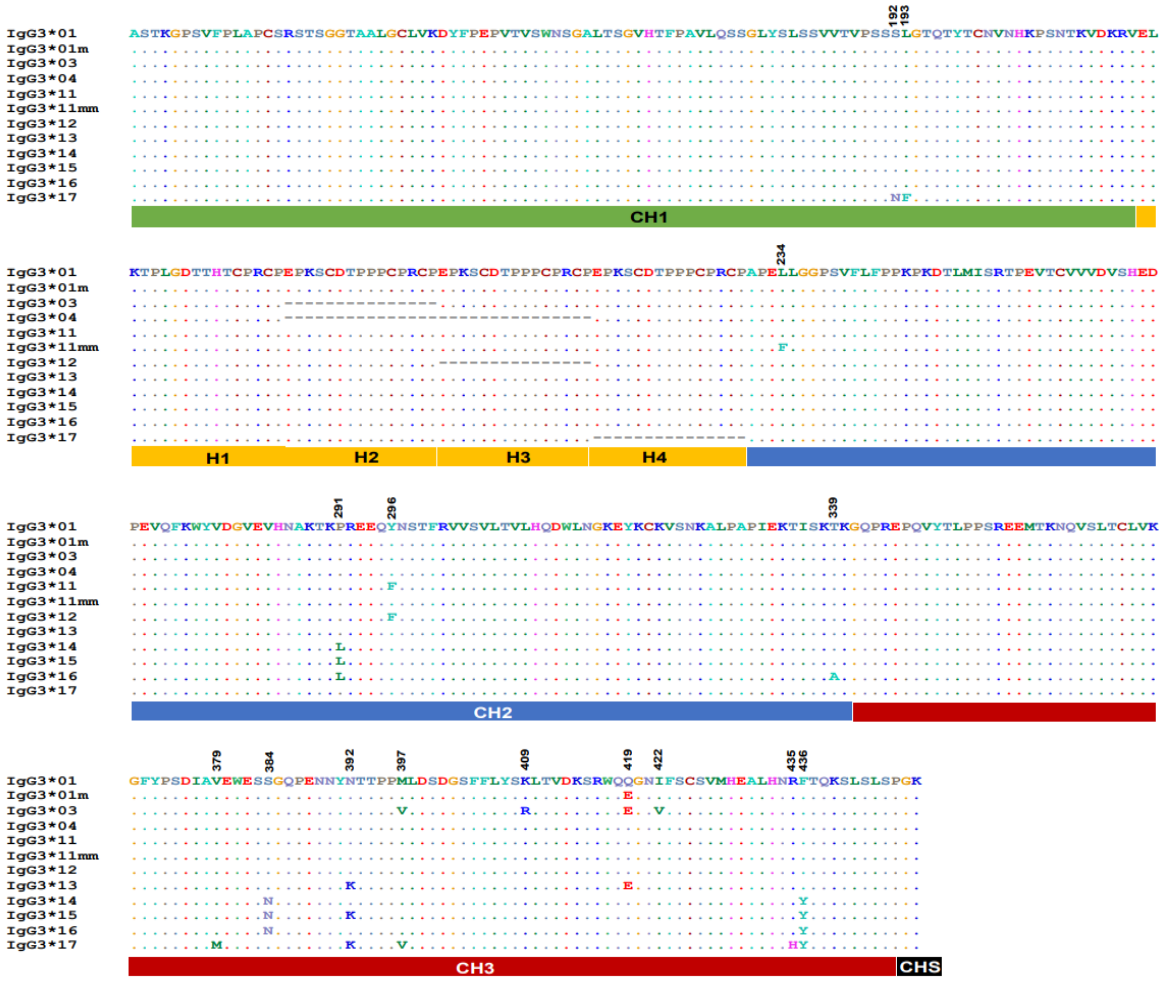

Figure 2. 1: Amino acid sequence alignments of IgG3 allelic variants. IgG3 allelic variants showing the constant regions [CH1(green), CH2 (blue), and CH3 (red) and the hinge H1-H4 (yellow) regions. The periods (.) denote sequence similarity to IgG3*01 whereas dashes (-) denote deletions in the hinge length of some IgG3 allelic variants. Amino acid sequence variations are shown for each domain. The Eu numbering shows the position of amino acids *(97)*.

2.3.1 Antibody Plasmid DNA Digestion

The constant heavy chain of *IGHG3*03*, *IGHG3*11* and *IGHG3*13* were present in CMVR expression plasmids of other HIV-specific antibodies. These variable genes required excision from the desired constant region containing plasmids. Heavy chain variable regions (VH-region) of these existing plasmids were swapped with the VH-region of CAP256-VRC26.25 *IGHG3*01*. The VH-regions were digested out of the plasmids using SalI and BshTI restriction enzymes (Figure 2.2), extracted and the VH-region of CAP256.25 *IGHG3*01* inserted into the plasmids following the protocol for plasmid DNA ligation. Briefly, for the digestion of these antibody plasmid DNAs, master mix was

prepared by adding 40 µL of dH_2O, 5 µL of universal buffer, 1.5 µL of BshTI (Thermo Scientific FastDigest), 1.5 µL of SalI (Thermo Scientific FastDigest) into a 200 µL PCR test tube. Two nanograms of plasmid DNA were added into each tube and incubated at 37ºC for 1.5 hours in the Thermocycler. To confirm complete plasmid digestion, 4 µL of each plasmid DNA digest and 5 µL of 1 kilobase pairs (kb) and 100 base pairs (bp) ladders (5 kb for plasmids and 400 bp for variable region) were loaded on 1% agarose gel, placed in an electrophoresis tank containing 1XTAE buffer and run for 30 minutes at 70 Volts. The gels were viewed under UV light (UV-Vilber Lourmet) and Bio-rad ChemiDoc™ XRS Imaging System (ChemiDoc™; Hercules, USA). Complete digestion was confirmed by matching the bands corresponding to the plasmids and the VH-regions to the1 kb and 100 bp DNA ladders. The remaining digest DNA were loaded on another 1% agarose gel and the backbone and heavy chains of *IGHG3*03*, *IGHG3*11*, *IGHG3*13* and CAP256-VRC26.25 *IGHG3*01* VH-region were cut out for extraction.

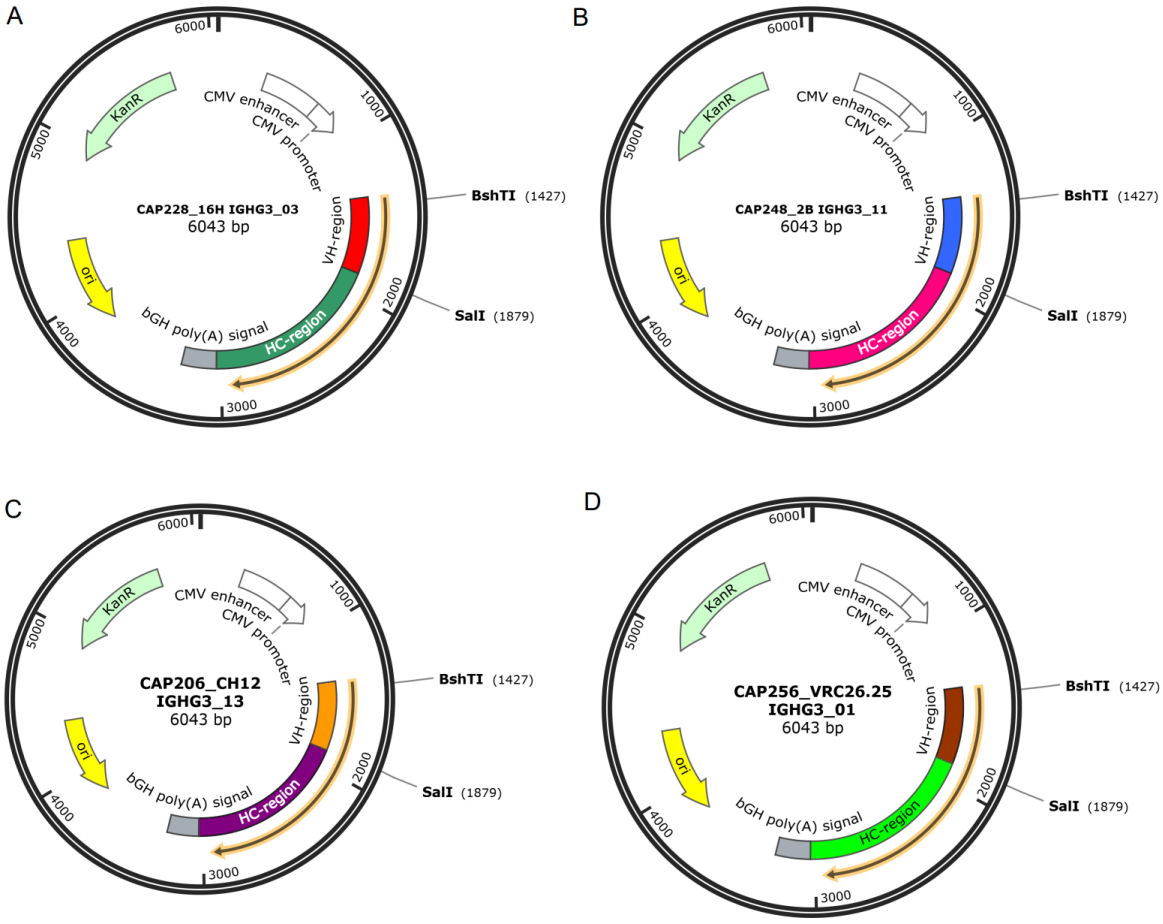

Figure 2. 2: Antibody plasmid digestion using restriction enzymes. The VH-region of (A) IGHG3*03, (B) IGHG3*11 (C) IGHG3*13 and (D) IGHG3*01 were cut out using SalI and BshTI restriction enzymes.

2.3.2 DNA Extraction (QIAquick Gel Extraction Kit Protocol)

Plasmids containing the constant heavy chain of *IGHG3*03*, *IGHG3*11* and *IGHG3*13* and the variable region (VH) of CAP256-VRC26.25 plasmids were cut out from the 1% agarose gel using a scalpel under UV light and extracted following the protocol described in the QIAquick Gel Extraction Kit (Qiagen Gmbh, Germany). The fragments were weighed in 1.5 mL microcentrifuge tubes. Three volumes of Buffer QG were added to one volume of the agarose gel containing the plasmid DNA and incubated at 50^{o}C for 10 minutes for the gel to melt while mixing every three minutes to enhance solubilization. Following solubilization, one volume of isopropanol was added to the DNA sample and mixed by inverting the tube. The DNA mixture was transferred to a QIAquick spin column and centrifuge at 13226 x g for one minute and the flow-through was discarded. The column was washed with 750 µL of Buffer PE and centrifuged at 13226 x g for one minute and the flow-through was discarded. The QIAquick column was centrifuged for an additional one minute to remove the remaining agarose or ethanol. The QIAquick column was then placed in a 1.5 mL microcentrifuge tube and 50 µL of elution Buffer EB (10 mM Tris-Cl, pH 8.5) was added at the center of the column and centrifuged at 6339 x g for two minutes. The concentration of the eluted DNA in the microcentrifuge tube was measured on the NanoDrop® ND-1000 Spectrophotometer (Wilmington, USA).

2.3.3 Antibody plasmid ligation

The Rapid DNA Ligation Kit (Roche Applied Science) was used to insert the VH-region of CAP256-VRC26.25 into the constant heavy chains. The amount of CAP256-VRC26.25 VH-region required for ligation into *IGHG3*03*, *IGHG3*11*, and *IGHG3*13* expression plasmids, was calculated using Promega Biomath calculator/DNA online tool (World.promega.com/resources/tools/biomath) to get a molar ratio of 3:1. Using an insert length of 0.458 kb and 5.5 kb of vectors, 4 ng of the insert and 15 ng of vector were pipetted into 200 µL PCR test tube containing 2.8 µL of dH_2O. Following was the addition of 2 µL of the ligation dilution buffer, 10 µL ligase buffer and 1 µL ligase. The solution was thoroughly mixed and incubated in the PCR machine at 25^{o}C for 30 minutes.

2.3.4 Plasmid DNA Transformation

The ligated plasmid DNA was transformed into XL10-Gold ultracompetent cells (Agilent Technologies, La Jolla, CA) following the manufacturers protocol. To introduce the

plasmid DNA into ultracompetent cells, 50 µL of the cells were transferred into pre-chilled 1.5 mL microcentrifuge tubes on ice. Following was the addition of 2 µL of β-mercaptoethanol, mixed and incubated for 10 minutes. This was followed by the addition of 2 µL of plasmid DNA and incubated for 30 minutes. The cells were heat-shocked at 42^{o}C in a water bath for 30 seconds. To help the bacteria recover quickly from the heat shock, 450 µL of super optimal broth with catabolite repression (S.O.C) (Invitrogen Life Technologies, Carlsbad, CA) was added to the tubes and incubated at 37^{o}C for 1 hour with shaking at 125 rpm. To grow colonies for miniprep, 50 µL of cell suspension was plated on Luria-Bertani (LB) agar containing 100 µg/mL Kanamycin at 37^{o}C overnight to allow for selection of the bacterial cells containing the plasmids to grow.

2.3.5 QIAprep Spin Miniprep kit (Qiagen, Hilden Germany)

A miniprep was performed for sequence confirmation of successful VH-regions swap. Two bacterial colonies were picked to increase the chances of getting one with the correct sequence and sub-cultured in 15 mL broth (10g of tryptone, 5g of yeast extract, 10g of NaCL , 25g of broth was dissolved in 1 liter of distilled water) (Sigma-Aldrich; St. Louis, USA) containing 100 µg/mL Kanamycin in 50 mL Falcon tubes and incubated at 37^{o}C overnight with shaking at 125 rpm for the bacteria to multiply and increase the plasmid DNA. The DNA was extracted using the QIAprep^{R} Spin Miniprep (Qiagen GmbH, Hilden Germany) following the manual procedure. Briefly, the broth cultures were spun down at 1957 x g for 15 minutes at room temperature and the supernatant was discarded. The pellet was resuspended in 250 µL Buffer P1 and then transferred into 1.5 mL microcentrifuge tubes. To lyse the cells, 250 µL Buffer P2 was added and mixed by inverting the tubes until the solution became clear. For binding of DNA, 350 µL Buffer N3 was added to neutralize and precipitate the genomic DNA, denatured cellular proteins and SDS prior to binding the DNA on the column and centrifuged for 10 minutes at 13226 x g. The supernatant was poured into QIAprep 2.0 spin columns and spun down for a minute. The bound DNA on the spin column was washed with 750 µL of Buffer PE, centrifuged for another minute and the flow-through discarded. The QIAprep 2.0 spin column was spun down for an additional minute to remove the residual wash buffer. The QIAprep 2.0 column was placed in a 1.5 mL clean microcentrifuge tube and 50 µL elution Buffer EB (10 mM Tris-Cl, pH 8.5) was added slowly at the center of the spin column, allowed to stand for a minute and centrifuged for one minute at 6339 x g. The

concentration of the DNA obtained was measured on the nanodrop instrument (NanoDrop® ND-1000 Spectrophotometer, Wilmington, USA).

2.3.6 Plasmid DNA Sequencing

IGHG3 DNA plasmid minipreps were sequenced using the BigDye™ Terminator v3.1 Cycle Sequencing Kit (Thermo Fisher Scientific; Waltham, USA) protocol. Multiple primers (Table 2.1) were used to create overlapping sequences covering the complete sequence of the alleles and ease of assembly of the fragments for sequence confirmation. Summarily, master mix was prepared by adding 1 µL BigDye Terminator (pink mix) ver3.1, 1.5 µL 5X BigDye^{TM} buffer, and 3.5 µL of dH_2O in a 200 µL PCR tube. Aliquots of the master mix were transferred into 200 µL strips or 96-wells microtiter plate. Three hundred nanograms of each *IGHG3* plasmid was pipetted into 200 µL strips or 96-well plate. Into the strips or wells containing each IGHG3 allele was added 3.2 picomoles of each primer. The mixture was incubated in the PCR machine at 25 cycles of 96^{o}C, 10 seconds, 50^{o}C, 5 seconds, 60^{o}C, 4 minutes, held at 4^{o}C.

Table 2. 1: Primer name and sequence for antibody plasmid DNA sequencing

Primer name	Primer sequence
CMVR F	5’-CTAGTTAACGGTGGAGGGCAGTGT-3’
HCRV	5’-CTTGTCCACCTTGGTGTTGC-3’
VHCH F01	5’-CACCTCTGGGGGCACAGC-3’
VHCH F02	5’-CCCAGCAACACCAAGGTGGACAAG-3’
CH2 F	5’-GGACCGTCAGTCTTCCTCTTCCC-3’
CH3 F	5’-CAGCCCCGAGAACCACAGGTG-3’

Sodium acetate was used for sequence clean-up. Fifty microliters of freshly prepared 4% sodium acetate (pH 5.2) in anhydrous ethanol (99%) (EtOH) was added to each 200 µL PCR tube or 96-wells plate and mixed thoroughly. The strips or plates were centrifuged for 30 minutes at 2000 x g, inverted, and centrifuged for an additional minute at 150 x g. Pellets were rinsed with 100 µL cold 70% ethanol, centrifuged for 5 minutes at 150 x g, inverted, centrifuged for one minute at 150 xg and then dried at 65^{o}C for three minutes in the PCR machine.

A 3500XL Genetic Analyzer (Applied Biosystems; Foster City, USA) was used to sequence the DNA samples and results exported as .AB1 files which were downloaded and imported into Sequencher version 5.4.6 DNA sequence analysis software (Gene

Codes Corporation, Ann Arbor, USA). Sequences were confirmed by assembling DNA fragments for overlapping sequences from the different primers and compared with the reference sequences from ImMunoGeneTics database (IMGT) and CAP256-VRC26.25 VH-region reference sequence. However, the sequences did not match due to the failure of the ligation enzyme to bind the insert to the heavy constant region and the plasmid.

2.3.7 Plasmid DNA cloning using NEBuilder

As an alternative approach to produce *IGHG3*03*, *IGHG3*11*, *IGHG3*13* expression plasmids and CAP256-VRC26.25 *IGHG3*01* VH-region, the NEBuilder HiFi DNA assembly kit and method (New England Biolabs Inc.) was used. The primers used for DNA amplification were: CMVR Forward, CMVR Reverse, G3 Apa Forward and G3 Apa Reverse (Table 2.2). CMVR reverse, G3 Apa forward were used to amplify the plasmid and the heavy constant domain while CMVR forward and G3 Apa reverse amplified CAP256-VRC26.25 VH-region. CMVR Forward and G3 Apa Forward were placed in the 5' prime ends in the plasmid and heavy constant domain while CMVR Reverse, and G3 Apa Reverse were placed at the 3' prime ends of the plasmid and heavy constant domain, respectively (Figure 2.3). In the NEBuider master mix, exonucleases removed the 5' ends of the plasmid to create 3' overhangs and the VH-region was annealed. DNA polymerase filled the gaps created in the 3' and ligase filled the nicks to produce the full heavy chain in the plasmid. Summarily, a reaction mixture was prepared by mixing 10.5 µL dH_2O, 0.5 µL forward (F) and reverse (R) primers, 4 ng plasmid DNA, 12.5 µL Q5 Hot start Master mix and 1 µL 5x buffer. The solution was thoroughly mixed and incubated for 25 cycles at 98^{o}C, 30 seconds; 98^{o}C, 10 seconds; 58^{o}C, 20 seconds; 72^{o}C, 2 minutes and an extension of 30 seconds for CAP256-VRC26.25 VH-region plasmid and four minutes for *IGHG3*03*, *IGHG3*11* and *IGHG3*13* plasmids. To confirm the successful plasmid DNA amplification, 4 µL of each reaction mixture was run on 1% agarose gel with 5 µL of 1 kb and 500 bp ladder and the bands obtained were of the required size and purity.

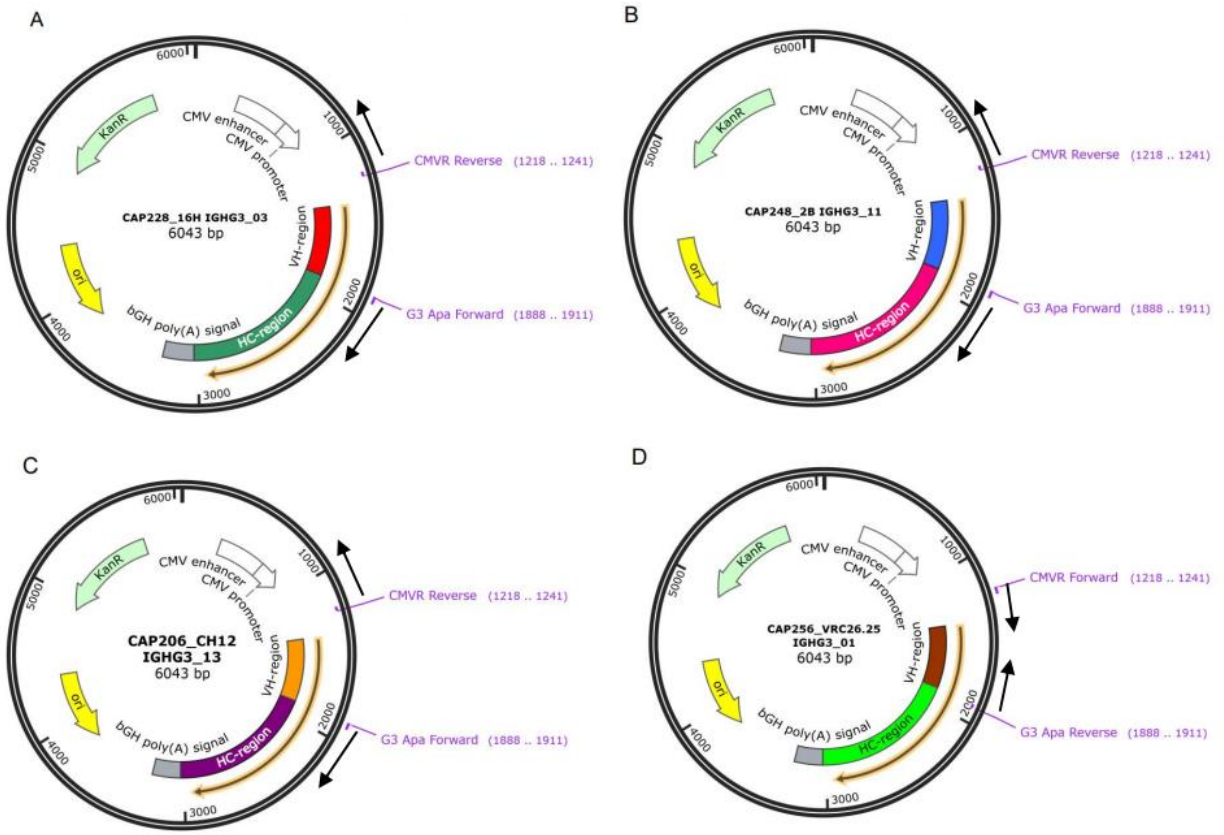

Figure 2. 3: Antibody plasmids and CAP256-VRC26.25 VH-region amplification using NEBuilder. A) *IGHG3*03* CMVR plasmid, B) *IGHG3*11* plasmid and C) *IGHG3*13* amplified with G3 Apa Forward and CMVR reverse primers. D) CAP256-VRC26.25 *IGHG3*01* VH-region amplified with CMVR forward and G3 Apa reverse primers.

Table 2. 2: Primer name and sequence for NEBuilder DNA cloning

Primer position	Primer name	Primer sequence
In the vector before signal sequence of VH-region	CMVR Forward	5'-CTAGTTAACGGTGGAGGGCAGTGT-3'
At the beginning of CH1	G3 Apa Forward	5'-GGGCCCATCGGTCTTCCCCCTGGC-3'
In the vector before signal sequence of VH-region	CMVR Reverse	5'-ACACTGCCCTCC ACCGTTAACTAG-3'
At the beginning of CH1	G3 Apa Reverse	5'-GCCAGGGGGAAGACCGATGGGCCC-3'

Following electrophoresis, a 10 µL reaction mixture was prepared by mixing 8 µL of each plasmid DNA to 1 µL of 10X CutSmart™ Buffer and 1 µL of Dpn I in a 200 µL PCR tube and incubated at 37°C for 30 minutes in a PCR machine to digest the parent DNA. Subsequently, the mixture was incubated at 80°C for 20 minutes in the PCR machine to inactivate Dpn I. The PCR products were assembled using the HiFi DNA assembly

protocol. Briefly, 10 µL of HiFi DNA assembly master mix, 8 µL of dH_2O, 1 µL of insert and 1 µL of backbone were placed in a 200 µL PCR tube and incubated in a thermocycler at 50^oC for 30 minutes. The exonucleases chewed back 5' ends, the insert annealed, DNA polymerase extended the 3' ends and DNA ligase sealed the nicks. The assembled product was used for transformation in XL10-Gold ultracompetent cells (Agilent Technologies, La Jolla, CA); following the transformation protocol.

Lastly, 2 µL of the assembled product was added to 50 µL XL10-Gold ultracompetent cells in pre-chilled 1.5 mL centrifuge tubes and mixed by flicking the tubes followed by incubation on ice for 30 minutes. The tubes were heat shocked at 42^oC for 30 seconds, transferred back on ice for two minutes, followed by addition of 950 µL room-temperature S.O.C media and incubated at 37^oC for 60 minutes with 250 rpm shaking. On LB agar plates containing Kanamycin, 100 µL of the cells were streaked on the plates and incubated overnight. To increase the probability of getting a colony with the insert, two colonies were picked from each plate and sub-cultured for Miniprep and sequencing as described in sections 2.3.5 and 2.3.6, respectively.

2.3.8 Site-directed mutagenesis

Two (*IGHG3*15* and *IGHG3*16*) of the twelve alleles studied were produced in-house from an available plasmid (*IGHG3*14*) in our laboratory by site-directed mutagenesis. *IGHG3*15* and *IGHG3*16* differ from *IGHG3*14* by a single nucleotide polymorphism (SNP). To make IgG3*15, a single mutation was introduced at position 392 in CH3 of IgG3*14 where asparagine (N) was mutated to lysine (K). To make IgG3*16 a single mutation was also introduced in IgG3*14 whereby Threonine (T) was replaced with alanine (A) at position 339 on CH2. The primers for mutation were designed following the guidelines in the QuikChange Lightning manual as shown in Table 2.3.

Table 2. 3: Forward and reverse primers used to make *IGHG3*15* and *IGHG3*16* from *IGHG3*14* by site-directed mutagenesis.

Plasmid DNA	Plasmid obtained	Primer name	Primer sequence
*IGHG3*14*	*IGHG3*16*	T339A F	5'-GAAAACCATCTCCAAAGCCAAAGGACAGCCCCG-3'
		T339A R	5'-CGGGGCTGTCCTTTGGCTTTGGAGATGGTTTTC-3'
*IGHG3*14*	*IGHG3*15*	N392K F	5'-GCCGGAGAACAACTACAAGACCACGCCTCCCAT-3'
		N392K R	5'-ATGGGAGGCGTGGTCTTGTAGTTGTTCTCCGGC-3'

Site-directed mutagenesis was performed using the QuickChange Lightning Site-Directed Mutagenesis Kit (Agilent Technologies; Santa Clara, USA) as per the manufacturer's protocol. A 50 µL reaction mixture was made containing 5 µL of 10X reaction buffer; 1 µL 50 ng plasmid DNA; 1 µL 125 ng forward primer; 1 µL 125 ng reverse primer; 1 µL dNTP mix; 1.5 µL QuickSolution reagent; 39.5 µL dH_2O; and 1µL QuickChange Lightning Enzyme. The reaction mixture was placed in a thermal cycler with the following parameters: 1 cycle of 95ºC, 2 minutes, 18 cycles of 95ºC, 20 seconds, 60ºC, 10 seconds, 68ºC, 4 minutes, 1 cycle of 68ºC, 5 minutes, held at 4ºC.

Two microliters of Dpn I restriction enzyme was added to each reaction mixture and incubated at 37ºC for two hours to digest the parent DNA completely. The DNA obtained post Dpn I digest was transformed as described in section 2.3.5.

2.3.9 Plasmid DNA Maxipreps

To maximize the plasmid DNA yield for transfection, a maxiprep was carried out. The sequence of antibody expression plasmids was confirmed as described in Section 2.3.6 for plasmid DNA sequencing. Plasmids were maxiprepped using the ZymoPURE™ II Plasmid Maxiprep Kit and protocol (Zymo Research Corp, Irvine, USA). Briefly, the transformation was carried out as previously described in Section 2.3.5 with the modification that picked colonies were plated in 150 mL of broth (Sigma-Aldrich; St. Louis, USA). After overnight culture, the broth cultures were centrifuged in falcon tubes at 6339 xg for 8 minutes.

Maxiprep was then performed as per the manufacturers protocol. Briefly fourteen milliters each of ZymoPURE™ P1, ZymoPURE™ P2 and ZymoPURE™ P3 were added to resuspend, lyse, and neutralize the mixture. The mixture was filtered into a 50 mL falcon tube using a ZymoPURE™ syringe. Fourteen milliters of ZymoPURE™ Binding Buffer was added and the mixture transferred into the Zymo-Spin™ V-P Column Assembly placed on a vacuum manifold (Sartorius stedim biotech, Bohemia, USA) to filter out the solution but retain the DNA on the column. Five milliters of ZymoPURE™ wash buffer 1 was added to the column to wash out the Binding Buffer and allowed to flow-through, followed by the addition of ZymoPURE™ wash buffer 2 to dissolve any residual Binding Buffer. The Zymo-Spin™ V-P Column was placed in a 2 mL centrifuge tube and spun down at 13226 x g for one minute to remove the residual wash buffer. The column was transferred into a clean 1.5 mL microcentrifuge tube and 200 µL ZymoPURE™ Elution

Buffer was added to the membrane of the column and allowed to stand for two minutes before centrifuging at 6339 x g for two minutes (modification from adding 400 µL of elution buffer at once). This step was repeated by the addition of another 200 µL ZymoPURE™ Elution Buffer. The concentration of the DNA obtained was measured on the Nanodrop (NanoDrop® ND-1000 Spectrophotometer; Wilmington, USA) and sequences were confirmed again as described previously in Section 2.3.6 except the CAP256-VRC26.25 lambda that was included in the sequencing reactions. Here, only the CMVR forward primer was used as coverage was adequate of the CAP256-VRC26.25 lambda chain. Using the forward vector primer CMVR F provides sequences of single strands (SS), variable and complete constant regions. Plasmids with confirmed sequences were transfected in HEK 293F cells.

2.4.0 Antibody Expression and Purification

2.4.1 Antibody transfection

Before transfection, human embryonic kidney (HEK) 293F cells were seeded in 400 mL FreeStyle™ media at $1x10^6$ cells/mL in one liter (1L) flask and placed in a shaking incubator (at 125 rpm) at 37°C, 10 % CO_2 and 70% humidity overnight to reach two million cells/mL before transfection. The heavy and light chain plasmids were co-transfected into HEK 293F cells (Thermo Fisher Scientific; Waltham, USA). One thousand two hundred microliters (1 mg/mL) of polyethylenimine (PEI) MAX 40,000 (Polysciences) was mixed with 10 mL Gibco Opti-Minimum Essential Medium (MEM) transfection reagent in a sterile 50 mL falcon tube and incubated for five minutes. In another 15 mL falcon tube, 200 µg each of heavy and light chain plasmid DNA were mixed in 10 mL Gibco Opti-MEM transfection reagent and incubated for five minutes. Following incubation, the Gibco Opti-MEM-DNA mixture was filtered into the 50 mL falcon tube containing PEI Max/Opti-MEM solution using a 0.22 µm filter and incubated for 20 minutes for the plasmid DNA to bind to PEI-Max. The mixture was transferred to the FreeStyle™ media containing HEK 293F cells (Thermo Fisher Scientific; Waltham, USA) slowly while shaking and incubated at room temperature for 20 minutes to allow the liposomes to enter the cells. The transfection mixture was incubated at 37°C, 10 % CO_2 and 70% humidity in a shaking incubator at 125 rpm for six days.

2.4.2 Antibody harvesting and purification.

The expressed monoclonal antibodies (mAbs) were harvested by transferring the culture supernatant into a 500 mL tube and spun down for one hour at 4^{o}C, 6000 x g. The supernatant was poured into a 0.22 µm “rapid”-Filtermax flask (TPP, Transadingen, Switzerland) and vacuum filter sterilized and purified using IgG column protein G (Thermo Fisher Scientific, Waltham, USA).

Protein G beads (Thermo Fisher Scientific; Waltham, USA) were mixed thoroughly and 4 mL was transferred into a 14 cm Bio-rad Econo-Pac column attached to a retort stand and allowed to settle to 2.5 mL and the column equilibrated with 10 column volumes of phosphate buffered saline (PBS). Protein G was used to selectively bind IgG3. The harvested supernatant was allowed to flow through the column and was subsequently washed with 10 column volumes of PBS. The mAbs were eluted using 12.6 mL glycine-HCL elution buffer (pH 2.5, 0.1 M glycine and 0.15 M HCl) into 1.4 mL neutralization buffer (12 g UntraPure TRIS; 80 mL dH_2O, 1 M HCl, pH 8). Each antibody was dialyzed overnight in 10% PBS in a 15 mL Pur-A-Lyzer^{TM} Mega Dialysis Kit (Sigma-Aldrich). The concentration was measured on the Nanodrop® instrument using the extinction coefficient for each antibody as determined using ProtParam (ExPASy) (https:web.expasy.org/protparam) following which 500 µL of the antibody was aliquoted into 1.5 mL cryotubes and stored at -70^{o}C.

2.5 Assessment of antibody purity and stability on sodium dodecyl-sulphate polyacrylamide gel electrophoresis (SDS-PAGE).

The sizes and purity of the mAbs were assessed by running a head-to-head SDS-PAGE using the NUPAGE kit and protocol (Thermo Fisher Scientific Inc). Briefly, 15 µL of each mAb was transferred into two 200 µL PCR tubes followed by the addition of 5 µL (1:4) of LDS sample buffer (NUPAGE^{R}). Three microliters of β-mercaptoethanol were added into the tubes for reduced mAbs. The tubes were placed in the thermocycler at 95^{o}C for five minutes to denature the quaternary structure of the antibody. Five microliters of each mAb and 10 µL of reference protein (ladder) were transferred into the wells of the gel and allowed to run for one hour at 80V. The gel was stained overnight in Coomassie blue and destained in 10% ethanal and 7.5% acetic acid then rinsed in distilled water to remove the excess dye. The electrophoresis bands on the gel were read using the Bio-Rad Imaging system (ChemiDoc^{TM}; Hercules, USA).

2.6 Pseudovirus transformation and sequence confirmation

This project made use of eight pseudoviruses (CAP256.2.00.C7J (PI), CA146.H3.3, CAP08.2.00.F6JC, CAP256.206sp.032.C9 (SU), 96ZM651.02, CAP84.32.2.00.32J, Q259.d2.17, and ZM249.1) to assess the neutralization potency and breadth of IgG3 allelic variants. Five (CAP8.6F, CAP84.32, Q259.d2.17, ZM249.1, and CAP256 SU) were already grown in-house and available in our laboratory. The maxiprep and backbone of two (CAP256 PI and 96ZM651.02) were available and CA146.H3.3 was transformed and maxiprepped. The envelope plasmid DNA was transformed into XL10-Gold ultracompetent cells (Agilent Technologies, La Jolla, CA) following the manufacturer`s protocol as described previously in section 2.3.10. Here, 100 µg/mL Carbenicillin was used instead of 100 µg/mL kanamycin and sequenced as described in section 2.3.6. A modification being the use of eight primers (Table 2.4) to create overlapping sequences that cover the entire length of gp160.

Table 2. 4: Primer name and sequence for CA146.H3.3 sequencing

Primer name	Primer sequence
Env B	5'-AGAAAGAGCAGAAGACATGGCAATGA-3'
A589	5'-GTGTAAAGTTAACCCCACTCTG-3'
A589 Rev	5'-CAGAGTGGGGTTAACTTTACAC-3'
Env A Rev	5'-TGCTGCTCCCAAGAACCCAA-3'
Env A Rev F	5'-TTGGGTTCTTGGGAGCAGCA-3'
E55	5'-GCCCCAGACTGTGAGTTGCAACAGATG-3'
Nf	5'-TGACCTGGATGCAGTGG-3'
Nr	5'-GGTGAGTATCCCTGCCTAACTCTA-3'

2.7 Pseudovirus Production

Pseudoviruses for neutralization assays were grown in HEK 293T cells. HEK 293T cells were seeded at six million cells/mL in 20 mL Dulbecco`s Modified Eagle Medium (DMEM) containing 10% fetal bovine serum (FBS), 2.5% 4-(2-hydroxyethyl)-1-piperazineeth anesulphonic acid (HEPES) and 0.5% gentamycin in a T75 flask the previous day. Five hundred microliters of DMEM (serum free) were mixed with 48 µL of Polyethylenimine (PEI) Max 40,000 followed by the addition of 8000 ng HIV-1 Env plasmid and 8000 ng pSG3Δenv backbone. The mixture was incubated for 20 minutes at room temperature, transferred to HEK 293T cells, and incubated at 37^{o}C with 5% CO_2 for 72 hours. The supernatant was filtered through a 0.45 µm filter and mixed with 20% (v/v) FBS and 1 mL

aliquoted into 1.5 cryotubes for storage at -80^{o}C. Tissue cell infectious dose ($TCID_{50}$) was measured after freezing for twelve hours.

2.8 Tissue cell infectious dose measurement ($TCID_{50}$)

$TCID_{50}$ was performed to determine the pseudovirus concentration that infects 50% of TZM-bl cells. A vial of the harvested virus was thawed to room temperature and 25 µL was added to 100 µL of DMEM in duplicate in a 96-well microtiter plate. A one in five (1 in 5) viral dilution was made and 25 µL transferred across from row A, to H, discarding 25 µL after the last dilution. TZM-bl cells were resuspended at $0.5x10^{6}$ cell/mL in DMEM growth medium and Dextran (40 µg/mL) at 14µL/mL and 100 µL transferred into wells of the plate containing the viruses. The plate was incubated at 37^{o}C with 5% CO_2 for 72 hours. One hundred microliters medium was removed and replaced with 100 µL firefly luciferase substrate (Bright-Glo, USA), incubated for two minutes and read using PerkinElmer Victor XLight Luminometer (PerkinElmer, Waltham, USA). Results were exported as Excel files and the relative light units (RLUs) were determined by the dilution with 50% infectivity.

2.9 Neutralization Assay

A neutralization assay (Table 2.5) was performed to assess the concentration of the mAbs that will block 50% of the viruses from infecting the TZM-bl cells as described by Montefiori (21). TZM-bl cells containing the firefly luciferase reporter gene is under the control of the HIV-1 long-terminal repeats (LTR) promoter region in which firefly luciferase is expressed only after viral infection. Neutralization activity was reported as a reduction in RLUs after a single round of pseudovirus infection in the presence of the bNAbs. The starting concentrations of CAP256-VRC26.25 antibodies were 5 µg/mL (CAP256 PI, 96ZM651.02, and CAP84.32) for a 3-fold dilution, 1 µg/mL (Q259.d2.17 and CAP8.6F) for a 3-fold dilution and 1 µg/mL (ZM259.1, CA146.H3.3 and CAP256 SU) for a 5-fold dilution. Following antibody dilution, 25 µL virus was added into the plate and incubated at 37^{o}C for one hour.

TZM-bl cells seeded at $0.5x10^{5}$ cells/ml for two days with ≥90% confluency were washed with 6 mL PBS and disrupted with 2.5 mL trypsin in a 125 mL flask. The cells were diluted to $0.5x10^{6}$ cells/mL, mixed with DEAE Dextran (40 µg/mL) and 20 µL of cells suspension was added to each well and incubated for 48 hours. After 24h hours of incubation, 130 µL of DMEM growth media was added to each well and incubated for

another 24 hours. After 48 hours of culture,100 µL of DMEM growth media was removed from each well, replaced with 100 µL of luciferase substrate and incubated for two minutes at room temperature. To determine the RLU for each antibody,150 µL of the mixture was transferred into 96-wells black microtiter plates and read using PerkinElmer Victor XLight Luminometer (PertkinElmer, Waltham, USA). To assess neutralization, 50% inhibition concentration (IC_{50}) was calculated as the dilution at which the infection was reduced by 50% compared to virus control without antibodies. All IgG3 allelic variants were run head-to-head on the same plate to limit intra-experimental variation. The results were exported as Excel files and copied into a macro-template for analysis.

Table 2. 5: Pseudovirus name, subtype and accession number used in the TZM-bl assay (sourced from https//:hiv.lanl.gov)

S/N	Virus name	Subtype	Accession number
1	CAP256.2.00.C7J [CAP256 (PI)]	C	EF203981
2	CAP256.206sp.032.C9 [CAP256 (SU)]	C	KF241776
3	CAP84.2.00.32J (CAP84.32)	C	EF203963
4	CAP08.2.00.F6JC (CAP8.6F)	C	EF203976
5	CA146.H3.3	C	JN681219
6	Q259.D2.17	A1	AF407152
7	96ZM651.02	C	AF286224
8	ZM249.1	C	DQ388514

2.10 Data Analysis

Sequences were analyzed using Sequencher 5.4.6 version. Statistical analysis was done on GraphPad Prism 8 (GraphPad Software; La Jolla, USA). Comparison between IgG3 antibodies was done using Friedman`s test for matching groups with Dunn`s correction. Confidence intervals were determined at 95% and $p<0.05$ or $p<0.001$ was denoted as significant.

3.0 Results

3.1 Optimization of digestion of *IGHG3* allelic variants heavy chain variable region

IgG3*03, IgG3*11 and IgG3*13 CAP256-VRC26.25 allelic variant plasmids were made using CAP228.16H *IGHG3*03*, CAP248 2B *IGHG3*11* and CAP206.CH12 *IGHG3*13* expression plasmid vectors by swapping VH-regions with the CAP256-VRC26.25 VH-region. To cut out the VH-regions, these plasmids were digested using SalI and BshTI restriction enzymes. Complete digestion was confirmed by running the plasmid digest on 1% agarose gel (Figure 3.1A). Bands numbered five to eight (5-8) (about 5341bp) confirmed the linearized plasmids and the heavy constant domain. Bands in lane 1 (about 452bp) and 2-4 (430bp) corresponding to the VH-regions were observed as expected (Figure 3.1A). The sizes of the plasmid and heavy constant domain were determined by comparing to a one kilobase ladder and the VH-regions using a 500 bp ladder. Following ligation, sequencing revealed that there was no VH-region inserted, suggesting that ligase didn`t seal the nicks between the backbone and the VH-region. Instead, only the backbone sequence was obtained even after ligation was repeated. While the gel shown in Figure 3.1A confirmed that digestion was successful, ligation was unsuccessful.

In order to overcome this, we used Q5 mastermix to amplify the plasmids and the heavy constant domain and the insert using forward and reverse primers in order to perform NEBuilder cloning. The purity and yield of the PCR product was confirmed by 1% agarose gel electrophoresis (Figure 3.1B). Lanes 3, 4 and 5 show *IGHG3*03*, *IGHG3*11* and *IGHG3*13* at about 5588bp as expected. Lane 2 represents CAP256-VRC26.25 VH-region of the desired size (about 650bp). The sizes were determined by comparing the bands to 100 bp (lane 1) and 1 kb (lane 6) ladders. The VH-region of CAP256-VRC26.25 was inserted into all the plasmids using NEBuilder HiFi DNA Assembly Master Mix and sequences confirmed.

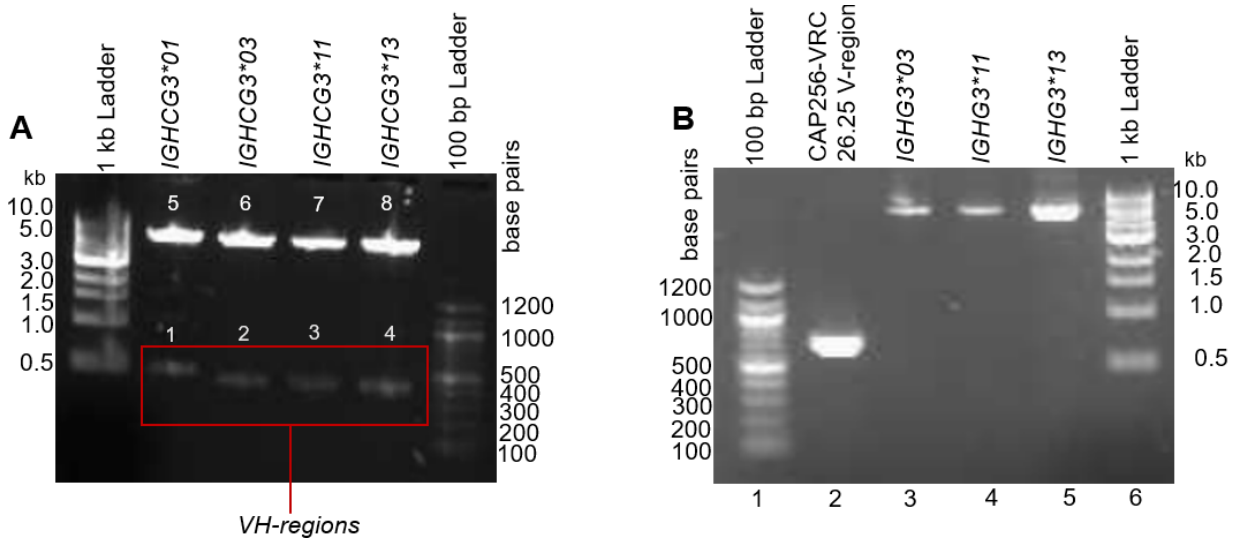

Figure 3. 1: Digested and amplified antibody plasmid DNAs. A) Plasmid digestion of CAP256-VRC26.25 IGHG3*01, CAP228.16H IGHG3*03, CAP248.2B IGHG3*11 and CAP206.CH12 IGHG3*13 using SalI and BshTI restriction enzymes. Bands (5-6) show plasmids and heavy constant domains of IGHG3*01, IGHG3*03, IGHG3*11 and *IGHG3*13*, respectively. Bands in the red box are the VH-regions of (1) CAP256-VRC26.25, (2) CAP22.16H, (3) CAP248.2B and (4) CAP206.CH12. One kilo base pair and 500 base pair ladders were used to determine the sizes. B) Plasmid DNA was amplified using the NEBuilder HiFi DNA assembly kit. Lane 2 shows CAP256-VRC26.25 VH-region and bands 3-5 represent *IGHG3*03*, *IGHG3*11* and *IGHG3*13,* respectively. Lanes one and six represent one kilo base pair and 500 base pair ladders were used to determine the sizes.

3.2 Sequence confirmation of engineered *IGHG3*15* and *IGHG3*16*

The amino acid sequences of IgG3*14, IgG3*15 and IgG3*16 allelic variants differ by single amino acid changes in the CH2 and CH3 domains. Mutations were introduced to IGHG3*14 by site-directed mutagenesis to produce *IGHG3*15* and *IGHG3*16*. In the IgG3*14 sequence, asparagine (N) was replaced by lysine (K) to make IgG3*15 and threonine (T) was replaced by alanine (A) to make IgG3*16 as shown in the confirmatory sequence chromatograms in Figures 3.2 (A) and (B).

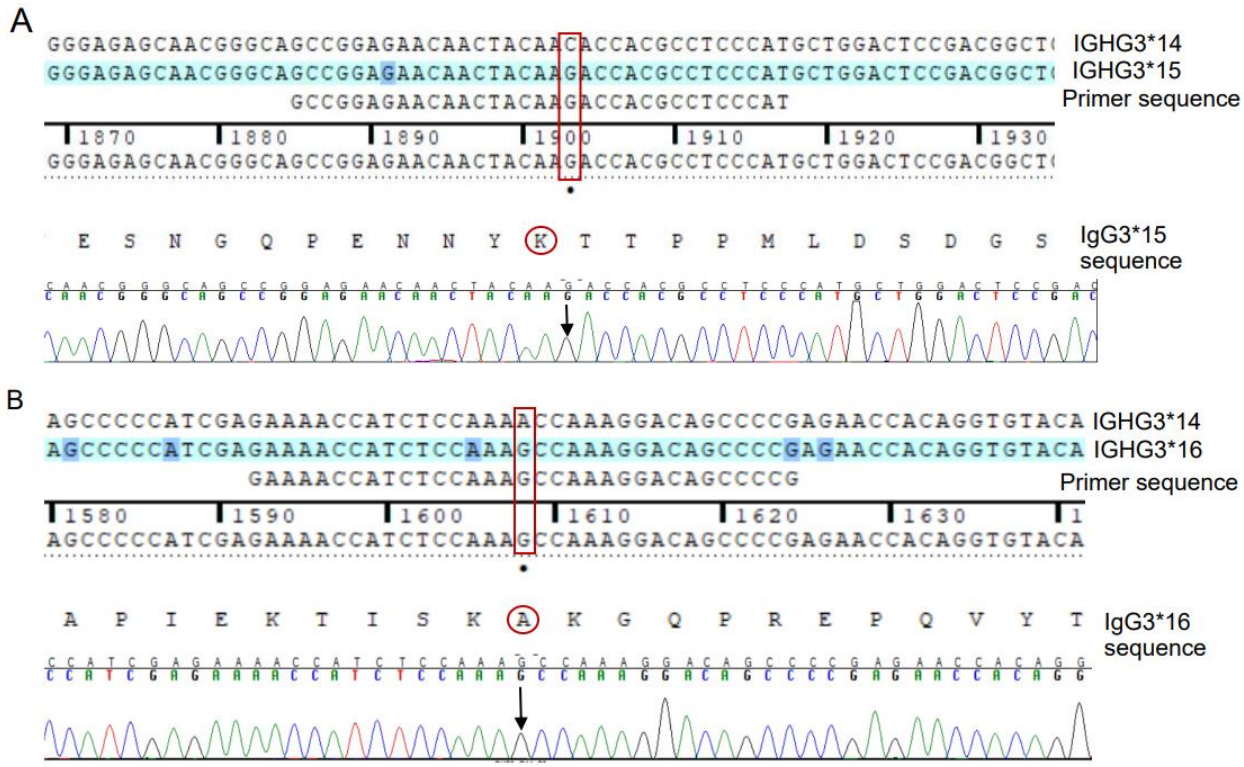

Figure 3.2: Site-directed mutagenesis: *A)* Site-directed mutagenesis of *IGHG3*14* to make *IGHG3*15* and *IGHG3*16.* The top sequence is *IGHG3*14*, and the middle sequence *IGHG3*15* and the last is the primer sequence used to make the mutation. The red box shows mutagenesis of "C" to "G. The chromatogram shows successful mutagenesis and amino acid substitution in the red circle where asparagine (N) in IgG3*14 is replaced with lysine (K) in IgG3*15. B) Site-directed mutagenesis of *IGHG3*14* to make *IGHG3*16*. The top sequence is *IGHG3*14*, and the middle sequence *IGHG3*16* and the last is the primer sequence used to introduce the mutation. The red box shows mutagenesis of "A" to "G". The chromatogram shows successful mutagenesis and the amino substitution in the red circle in which threonine (T) in IgG3*14 is replaced with alanine (A) in IgG3*16.

3.3 Expression and yields of IgG3 allelic variants

The sequences of the eleven IgG3 allelic variants were confirmed and the heavy and lambda light chains of the antibody plasmid DNA were co-infected in HEK293F cells, harvested and purified by Protein G chromatography. IgG3*17 was available already expressed. The concentrations and yields were measured (Table 3.1) and the antibodies were aliquoted and stored at -70^{o}C. The maximum yield was IgG3*15 measuring 7.88 mg and the minimum yield of IgG3*14 measuring 2.70 mg. However, all yields obtained were enough for downstream experiments. The amino acid sequence of IgG3*14 differed from IgG3*15 and IgG3*16 by one amino acid, suggesting that this single change might have

influenced expression, however further head-to-head expressions would be required to confirm this.

Table 3. 1: IgG3 allelic variant expression yields. Extinction coefficient used to calculate the concentration as determined by ExPASy, concentration as determined by nanodrop and yield as volume multiplied by concentration.

Antibody	Extinction Coefficient	Concentration (mg/ml)	Yield (mg)
IgG3*01	15.08	1.06	5.83
IgG3*01m	15.08	1.02	3.57
IgG3*03	15.37	1.06	5.30
IgG3*04	15.66	0.95	2.85
IgG3*11	14.90	0.97	4.37
IgG3*11mm	15.03	0.92	5.06
IgG3*12	15.22	0.91	3.64
IgG3*13	15.31	0.98	4.41
IgG3*14	15.25	1.08	2.70
IgG3*15	15.25	1.05	7.88
IgG3*16	15.26	0.98	4.41

3.4 Quality control confirming the size and stability of IgG3 allelic variants on sodium dodecyl-sulfate polyacrylamide gel electrophoresis (SDS-PAGE).

The expressed and purified IgG3 allelic variants as well as the CAP256-VRC26.25 IgG1 control were assessed for purity and stability by running a head-to-head on SDS-PAGE gel (Figure 3.3). These were loaded with both non-reduced (NR) and reduced (R) forms of all antibodies alongside the pre-stained protein ladder to compare the sizes and purity of the mAbs and in the reducing condition to compare the sizes of the heavy and light chains. IgG3 allelic variants were found to be larger than IgG1 as expected. The molecular weight of non-reduced form of IgG3 occurred at approximately 170 kDa while that of IgG1 is 150 kDa due to its short hinge region of 15 amino acids (76). In the non-reduced condition, several bands can be noted beyond the full antibody at approximately 170 kDa and 150 kDa. These may correspond to different glycosylation profiles of the antibody, incomplete denaturation leaving the mAbs in their globular conformation which travel faster on the gel or due to fragmentation or small amounts of aggregation (98). In the reduced form, the heavy and light chains were separated by breaking the interchain disulphide bonds linking the two chains with beta-mercaptoethanol. The molecular weight of the heavy chains of IgG3 allelic variants was between 50 to 60 kDa while that of IgG1

was between 40 to 50 kDa as expected. However, some antibodies with reduced hinge lengths as a result of fewer hinge repeats such as IgG3*03, IgG3*12, IgG3*17 (three hinges) and IgG3*04 (two hinges) were slightly lower. The molecular weight of IgG3*04 heavy chain with two hinges was the closest to IgG1 heavy chain. The molecular weight of the lambda light chain was between 25 to 30 kDa since all mAbs used the same lambda light chain plasmid.

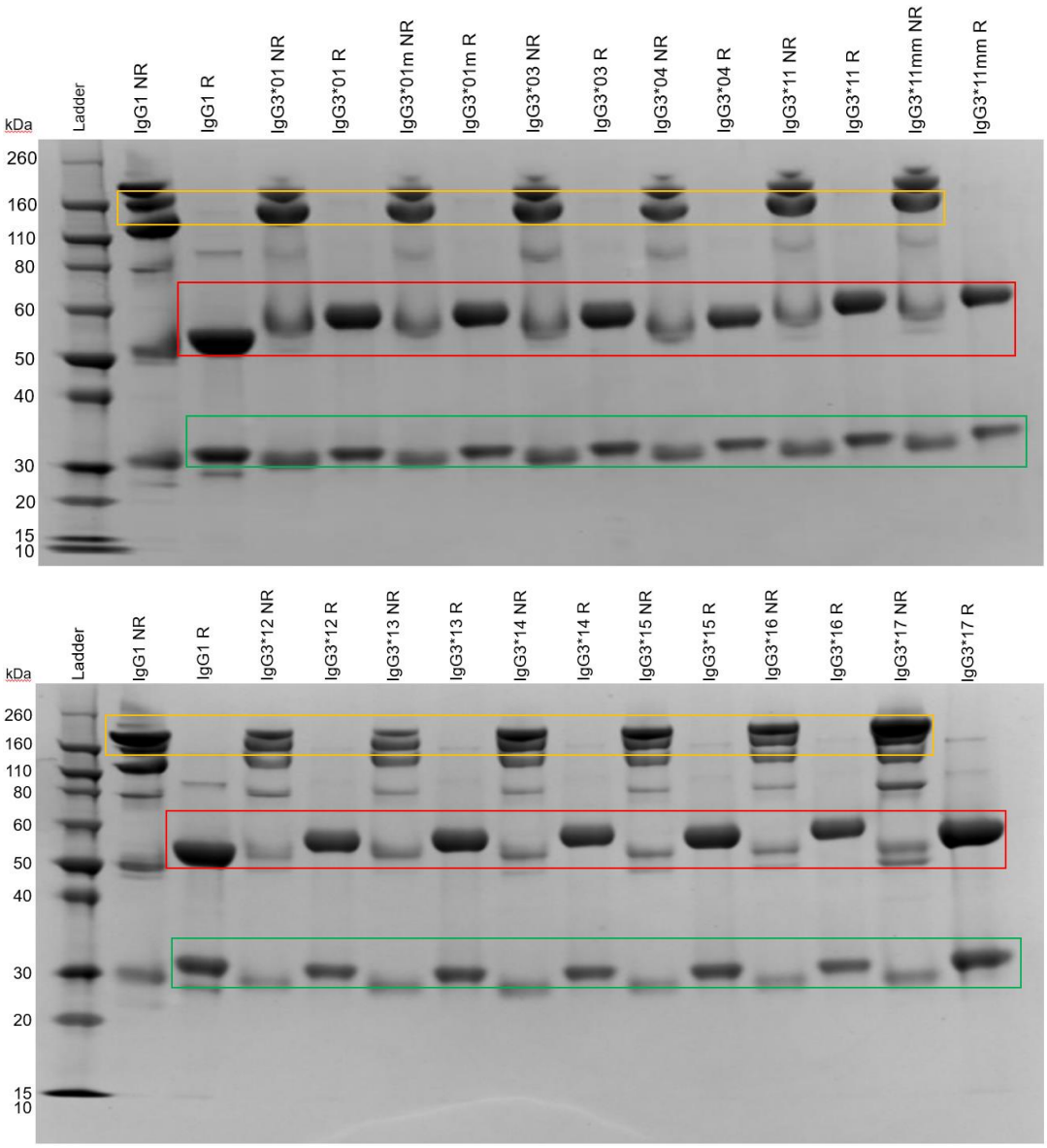

Figure 3.3: SDS-PAGE of IgG3 allelic variants: Head-to-head SDS-PAGE of non-reduced (NR) and reduced (R) forms of IgG3 allelic variants. The yellow box represents the non-reduced forms of each antibody, red box the heavy chains and the green box the lambda light chains. Extra bands in non-reduce form show incomplete denaturation or aggregations. Antibody sizes are determined using reference bands on the ladder by the side of each gel.

3.5 The impact of IgG3 allelic variants on neutralization

The mAbs were tested for neutralization against a panel of eight pseudoviruses. These viruses were chosen because they were more sensitive to CAP256-VRC26.25 IgG3*01 compared to CAP256-VRC26.25 IgG1 (45) with the exception of CAP256 SU. To assess the neutralization potency of the antibodies against the panel of viruses tested, the percentage inhibition was plotted against the antibody concentration (µg/mL) (Figure 3.4). Overall, the titration curves showed that IgG3*01 version (red) was higher than IgG1 (black) indicating enhanced potency. The largest difference between IgG3*01 and IgG1 was observed in CAP256 PI, 96ZM651.02 and CA146.H3.3. However, neutralization of some viruses such as CAP84.32, ZM249.1 and CAP256 SU by other IgG3 allelic variants was similar or equal to IgG1. There were subtle differences in the curves between IgG3 allelic variants, but all variants regardless of subtype neutralized the entire panel.

Using the titration curves as shown in Figure 3.4, we next determined the 50% inhibition concentration (IC_{50}) of all the variants (Table 3.2). All antibodies had an IC_{50} less than 1.5 µg/mL with Q259.d2.17, ZM249.1, CA146.H3.3 and CAP256 SU being the most sensitive viruses to CAP256.VRC26-25 variants. The most potent IgG3 variants measured as the geometric mean titer (GMT) across all viruses were IgG3*01, IgG3*01m, IgG3*13 and IgG3*14 (0.00001 – 0.0090 µg/mL). Overall, all IgG3 variants were more potent (<0.021 µg/mL) than IgG1 (0.05369 µg/mL).

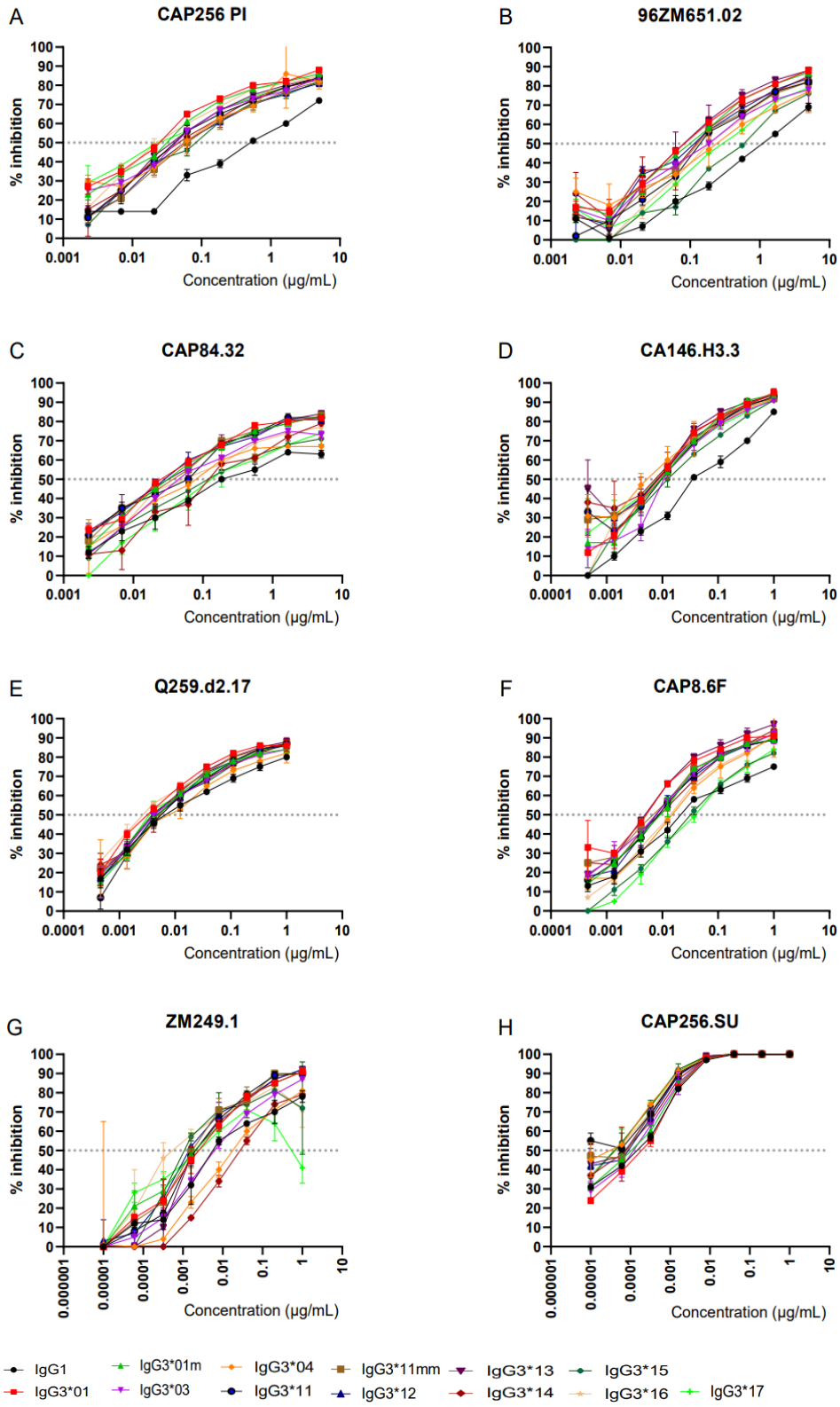

Figure 3.4: Neutralization of a panel of eight pseudoviruses. The dotted lines show the point on the curve corresponding to the IC_{50} of each antibody. Error bars represent the standard deviation of two repeats.

Table 3. 2: Neutralization potency of CAP256-VRC26.25 IgG3 allelic variants against a panel of eight pseudoviruses. Assessed by the TZM-bl neutralization assay, the values represent 50% inhibition concentration (IC_{50}). The geometric mean titer (GMT) gives the mean concentration of each antibody against all the viruses.

	Viruses								
mAbs	CAP256 PI	96ZM651.02	CAP84.32	CA146.H3.3	Q259.d2.17	CAP8.6F	ZM249.1	CAP256 SU	GMT
IgG1	0.44522	1.25811	0.17898	0.04949	0.00638	0.33091	0.00589	0.00112	0.05369
IgG3*01	0.01356	0.08422	0.02225	0.00554	0.00290	0.02135	0.00204	0.00048	0.00735
IgG3*01m	0.02178	0.09341	0.02832	0.00736	0.00512	0.03015	0.00211	0.00048	0.00951
IgG3*03	0.02264	0.13681	0.03940	0.00727	0.00459	0.07300	0.00429	0.00033	0.01198
IgG3*04	0.03465	0.16373	0.14003	0.00705	0.00831	0.22738	0.00905	0.00038	0.02087
IgG3*11	0.02445	0.10289	0.04707	0.00997	0.00409	0.04606	0.00316	0.00079	0.01238
IgG3*11mm	0.03238	0.11704	0.03424	0.00871	0.00394	0.04183	0.00204	0.00064	0.01118
IgG3*12	0.03077	0.10344	0.02397	0.00868	0.00383	0.04041	0.00215	0.00049	0.01010
IgG3*13	0.02066	0.07503	0.03029	0.00653	0.00304	0.03259	0.00185	0.00037	0.00822
IgG3*14	0.03149	0.10641	0.04034	0.00573	0.00532	0.07662	0.00162	0.00014	0.00956
IgG3*15	0.06355	0.33040	0.07472	0.01699	0.00385	0.17115	0.00274	0.00051	0.01990
IgG3*16	0.02054	0.13286	0.03628	0.00953	0.00333	0.07070	0.00165	0.00027	0.01000
IgG3*17	0.02346	0.21072	0.09896	0.00809	0.00361	0.06962	0.00124	0.00050	0.01255

Most potent → least potent

0.00001 – 0.0090	0.0100 – 0.0999	0.1000 – 0.3999	0.4000 – 0.9999	1.0000 – 1.5000	µg/mL

To assess the effect of class switch between IgG subclasses, a fold change was compared between IgG3 allelic variants relative to IgG1 against the virus panel. All IgG3 allelic variants had median values greater than one indicating that IgG3 versions were more potent than IgG1(Figure 3.5a). The largest difference relative to IgG1 (32.8-fold) was against CAP256 PI by IgG3*03 and the least (0.7-fold) against ZM249.1 by IgG3*04. This range of variability between viruses may suggest the presence of viral signatures that define if IgG3 were more potent than IgG1. However, to identify these, a significantly expanded virus panel will be required.

IgG3*01 had the highest median fold difference (8.0) relative to IgG1, indicating that it was the most potent version of CAP256-VRC26.25. The fold differences of IgG3*01 were significantly different to both IgG3*04 ($p = 0.0038$ which corresponded to the variant closest to IgG1 in neutralization) and IgG3*15 ($p = 0.0013$) which corresponded to the second least potent IgG3*3 allelic variant. IgG3*13, which showed similar fold differences to IgG3*01 was also significantly different from IgG3*04 ($p = 0.01570$) and IgG3*15 ($p = 0.0059$). When arranged by hinge length known to impact the neutralization capacity of IgG3 (45,46), IgG3*04 had the lowest fold difference from IgG1, also had the fewest number of hinges (two) potentially making it similar to IgG1 in flexibility. However, IgG3*15 had substantially lower fold differences as compared to other allelic variants with four hinges, suggesting that neutralizing potency is not influenced by hinge length alone

Comparison between the novel alleles (IgG3*01 versus IgG3*01m and IgG3*11 versus IgG3*11mm) did not show any significant differences indicating that these novel alleles do not impact on neutralization.

We next visualized the data by comparing fold changes relative to IgG3*01 to assess the neutralization potency within IgG3 allelic variants (Figure 3.6b). The largest median fold change (7.6) within IgG3 allelic variants was observed in IgG3*13 relative to IgG3*01 against CAP256 SU and the least median fold change (2.2) was observed in IgG3*04 against ZM249.1 and CAP84.32. Overall, IgG3 allelic variation only slightly impacts the neutralization in contrast to the comparatively larger differences seen for a subclass switch from IgG1. All median fold difference values were less than one, indicating that IgG3*01 was more potent compared to the rest of the IgG3 allelic variants. IgG3*13 had the highest median fold differences, closest to 1 (0.9-fold) whereas IgG3*15 and IgG3*04 had the lowest median fold differences (0.3-fold). Among the IgG3 allelic variants, there was a significant difference between IgG3*13 and IgG3*15 ($p = 0.0030$) and IgG3*13 and IgG3*04 ($p = 0.0141$) as determined by the Turkey`s multiple comparison test. IgG3*13 and IgG3*15 were significantly different despite both having 4 hinges translating to the same hinge length. When antibodies with three hinges were compared, IgG3*12 had the highest median fold difference (0.8-fold) meanwhile IgG3*03 and IgG3*17 were similar (0.6 and 0.7-fold respectively). IgG3*04 has two hinges and had the lowest median fold difference (0.3-fold). This suggests that beyond the hinge length known to impact the neutralization potency of CAP256-VRC26.25 (45), sequence differences beyond this region are likely to have an effect. Overall, while IgG3*13 showed improvement over IgG3*01 against some viruses (CAP256 SU and ZM249.1), none of the IgG3 allelic variants overall were improved above IgG3*01, but IgG3*04 and IgG3*15 were significantly worse. This confirms that amino acid variation in the IgG3 constant region can have significant impacts on the neutralization capacity of the antibody. When the hinge lengths were compared, there was a significant difference between 4 vs 2 hinges ($p=0.0483$) relative to IgG1 (figure 3.5c), 4 vs 2 hinges ($p=0.0471$) and 3 vs 2 hinges ($p=0.0014$) relative to IgG3*01 (figure 3.5d).

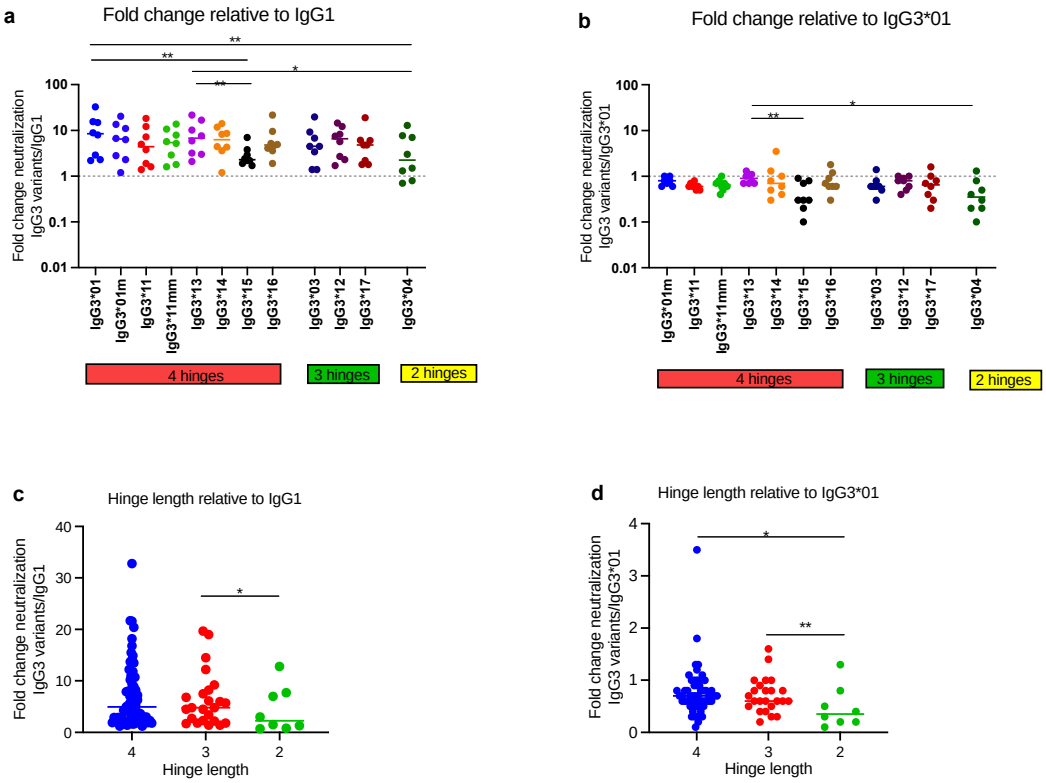

Figure 3.*5:* IgG3 allelic variation impacts neutralization of CAP256-VRC26.25 *a*) Neutralization fold change of IgG3 allelic variants relative to IgG1. The dotted line shows no fold change between IgG3 allelic variants and IgG1. The horizontal lines represent significant differences between IgG3 allelic variants and IgG1. b) Neutralization fold change of IgG3 allelic variants relative to IgG3*01. The dotted line shows no fold change (fold change = 1) between IgG3 allelic variants and IgG3*01. The horizontal lines represent significant differences between IgG3 allelic variants and IgG3*01. Significant differences were calculated using Friedman`s test for matching groups with Dunn`s correction. The confidence interval was set at 95%. Where *p<0.05 and **p<0.001. c) Comparison of hinge lengths relative to IgG1 d) Comparison of hinge lengths relative to IgG3*01. The horizontal line represents significant differences determined by Turkey`s multiple comparison test. Where *p<0.05; **p<0.001.

4.0 Discussion

In this study, we showed that IgG3 allelic variants of CAP256-VRC26.25 had more potent neutralization activity than the IgG1 variant. We used available sequence data from the HIV-1 CAPRISA 002 Acute Infection cohort and expressed the CAP256-VRC26.25 bNAb as IgG3 allelic variants that were previously found in the germline repertoire of these African individuals. The most potent of the IgG3 allelic variants was IgG3*01 meanwhile IgG3*04 and IgG3*15 were the least potent when compared to IgG1. While IgG3*04 has only 2 hinges compared to IgG3*01, IgG3*15, which does not differ in hinge length differs by several amino acids, indicating that both hinge length and amino acid differences in the IgG3 constant region contribute to altered neutralizing capacity of antibodies.

We confirmed that all IgG3 allelic variants showed improved neutralization activity compared to IgG1. This is consistent with previous studies from our laboratory that measured the neutralization activity of IgG3*17, IgG3*01 and novel allelic variant IgG3*01m versions of CAP256-VRC26.25 compared to IgG1 against a 50 virus panel (45). Other studies have also shown that IgG3 variants of NAbs were significantly more potent or of similar potency to their IgG1 counterparts (83,99,100) and suggest that isotype switching is a powerful engineering tool for improving the neutralization capacity of antibodies. This highlights the impact of the constant region on neutralization potency due to differences in amino acid sequences or hinge lengths influencing antibody-antigen binding.

The study further shows that allelic variation in IgG3 significantly impacted on the ability of CAP256-VRC26.25 to neutralize. We have previously shown that IgG3*01, IgG3*01m and IgG3*17 expressed as CAP256-VRC26.25 bNAbs showed improved neutralization, ADCP and ADCT compared to IgG1 (45). Further, there were subtle differences between IgG3 variants, where we observed lower levels of ADCC activity by IgG3*17 compared to the other variants attributed to a lysine at position 392 that abrogates a potential N-linked glycan (PNG) motif. ADCP, ADCT and neutralization potency was also different between allelic variants, the mechanism of which was determined to be primarily explained by IgG3*17 differing from IgG3*01 and IgG3*01m by a shorter hinge length (45). The allelic effect however may not be true for all antibodies. Others looked at allotypic variants of IgG3 and found no difference in the ability to neutralize by VRC01 (101). Several studies have shown differences in Fc effector function as a result of allelic variation and in the

case of IgG3, particularly the effect of the hinge length, something that is planned for future work on these antibodies (45,46).

This study gives some insight into the mechanisms through which allelic variation may affect neutralization. Between the IgG3 variants, there was a significant difference in neutralization between IgG3*01 and IgG3*04 that have the same sequence but differ by hinge lengths of four and two, respectively. As suggested by our previous studies, the longer hinge lengths were more potent at neutralization, perhaps as a result of more flexibility between the Fab and Fc regions and an increased angle between the Fab arms which may help the antibody penetrate the glycan shields (45,46). While this made an impact on neutralization in this study, it is likely to also impact the ADCP activity of these variants (45,46), however, this requires more study. These differences in neutralization however cannot be explained by hinge length alone. IgG3*11 (four hinges) and IgG3*12 (three hinges) are different only by hinge length but there was no significant difference in the neutralization potencies. Beyond this, IgG3*15 was significantly different from all other IgG3 variants with four hinges, again supporting that hinge length alone does not explain the effect completely. In addition, although there was no significant difference between allelic variants with three hinges, IgG3*12 showed improved neutralization, indicating that other factors contributed to this observation.

Beyond the hinge length, sequence differences between the IgG3 variants may account for some of the neutralization differences. IgG3*15 with the neutralization potency closest to IgG1 differs from IgG3*14 and IgG3*16 by the amino acid K392N resulting in a loss of a potential N-linked glycosylation site in IgG3*15. IgG3*16 also differs from IgG3*15 at position 339 but as this difference is also present relative to IgG3*14 where neutralization is similar, this indicates that the presence of alanine (A) in IgG3*16 is unlikely to have influenced enhanced neutralization potency. The K392N site is also present in IgG3*13 and IgG3*17 but in combination with a number of other mutations suggesting that the difference between IgG3*15 and IgG3*13 is not explained by K392N alone. K392N does have significant implications on Fc effector function, where we showed it resulted in reduced ADCC of CAP256-VRC26.25 IgG3*17 (45). This site has also been associated with differences in ADCC in other studies (102) and antibody stability (103) which may explain its effect on neutralizing IgG3*15.

The novel *IGHG3* alleles described in this study (IgG3*01m and IgG3*11mm) that were previously identified in African individuals did not show a significant difference when compared to IgG3*01 and IgG3*11 respectively, indicating no effect on neutralization potency of CAP256-VRC26.25. IgG3*01 and IgG3*01m differ by Q419E in the CH3 domain and IgG3*11 and IgG3*11mm differ by F234L and F296Y in CH2 which did not impact on function. These differences are, however, close to the Fc receptor binding sites for FcγRIIa (66), indicating that they may show a difference in ADCP function. In another antibody, IgG3*11mm showed enhanced ADCP compared to IgG3*01 but was not compared to IgG3*11 (96).

Several viruses showed greater neutralization differences between allelic variants than others. All viruses were more sensitive to IgG3 allelic variants compared to IgG1 except Q259.d2.17 and ZM249.1 against which the IgG3*04 variant was less sensitive compared to IgG1. While our previous study showed that CAP256.VRC26.25 IgG3 variants show enhanced neutralization in viruses lacking a potential N-linked glycan (PNG) motif at position 160, other viral signatures for this have not been delineated but require neutralization against a large panel of viruses (45). It is possible that viral signatures may also differentiate the neutralization activity of allelic variants.

Limitations

One of the limitations of our study is that we used only one bNAb targeting the V1/V2 site. It is not clear whether the allelic changes and effects will more broadly apply to other bNAbs. The panel of viruses used was small, and therefore viral signatures of IgG3 allelic variant differential neutralization could not be defined within this study. We will expand the panel of pseudoviruses for this reason in future studies. We were unable to determine the effect of Fc mutations on Fc effector functions due to time constraint, but such experiments should be included in future studies.

Conclusion

Studies aimed at developing preventive HIV vaccine focusing on the induction of broadly neutralizing antibodies have until now proven unsuccessful. However, passive immunization of bNAbs shows promise for HIV prevention and therapy. Our study explores the use of natural allelic variation in the constant region to improve neutralization potency of CAP256-VRC26.25. Our data suggest that producing mAbs as IgG3 with an extended half-life for preventive and clinical use should be considered and indicates that small allelic variations in the constant regions can have significant impacts on the neutralization capacity of antibodies.

The engineering of antibodies for passive immunization is mainly focused on IgG1 because of its long half-life of 21 days as compared to seven days of IgG3 and the relative ease of manufacture (32). However, several IgG3 allelic variants are known to have improved half-life including IgG3*17 (70). We previously showed that the type of light chain used for FcRn receptor binding depends on the pH. We showed that IgG3 variants using the lambda light chains binds to FcRn receptor at low pH, thus prolonging its half-life (83). Therefore, there are mechanisms to potentially overcome the undesirable short half-life of IgG3, which may enable their future use in passive immunization. This study further extends the promise of IgG3 for use in bNAb engineering to improve neutralization with specific focus on using natural allelic variation to enhance these functions. Therefore, selection of antibodies for passive immunization or therapy should consider the antibody subclass with enhanced properties such as potency and long half-life. This will reduce the incidence of HIV, leverage treatment compliance, increase individual income and improve our economy.

References

1. Pneumocystis Pneumonia --- Los Angeles [Internet]. [cited 2023 Feb 25]. Available from: https://www.cdc.gov/mmwr/preview/mmwrhtml/june_5.htm

2. Balatif R, Harahap H, Dhiyah I. Recent Development on HIV Variants and HIV Vaccine. Cermin Dunia Kedokt. 2022 Dec 19;49.

3. Bekker LG, Tatoud R, Dabis F, Feinberg M, Kaleebu P, Marovich M, et al. The complex challenges of HIV vaccine development require renewed and expanded global commitment. Lancet Lond Engl. 2020 Feb 1;395(10221):384–8.

4. Kumar S, Batra H, Singh S, Chawla H, Singh R, Katpara S, et al. Effect of combination antiretroviral therapy on human immunodeficiency virus 1 specific antibody responses in subtype-C infected children. J Gen Virol. 2020;101(12):1289–99.

5. Fact sheet - Latest global and regional statistics on the status of the AIDS epidemic. | UNAIDS [Internet]. [cited 2023 Aug 12]. Available from: https://www.unaids.org/en/resources/documents/2023/UNAIDS_FactSheet

6. Ng'uni T, Chasara C, Ndhlovu ZM. Major Scientific Hurdles in HIV Vaccine Development: Historical Perspective and Future Directions. Front Immunol. 2020 Oct 28;11:590780.

7. data-book-2022_en.pdf [Internet]. [cited 2023 Feb 25]. Available from: https://www.unaids.org/sites/default/files/media_asset/data-book-2022_en.pdf

8. Gao F, Weaver EA, Lu Z, Li Y, Liao HX, Ma B, et al. Antigenicity and immunogenicity of a synthetic human immunodeficiency virus type 1 group m consensus envelope glycoprotein. J Virol. 2005 Jan;79(2):1154–63.

9. Rudometov AP, Chikaev AN, Rudometova NB, Antonets DV, Lomzov AA, Kaplina ON, et al. Artificial Anti-HIV-1 Immunogen Comprising Epitopes of Broadly Neutralizing Antibodies 2F5, 10E8, and a Peptide Mimic of VRC01 Discontinuous Epitope. Vaccines. 2019 Aug 6;7(3):83.

10. Kwong PD, Wyatt R, Robinson J, Sweet RW, Sodroski J, Hendrickson WA. Structure of an HIV gp120 envelope glycoprotein in complex with the CD4 receptor and a neutralizing human antibody. Nature. 1998 Jun 18;393(6686):648–59.

11. Wyatt R, Kwong PD, Desjardins E, Sweet RW, Robinson J, Hendrickson WA, et al. The antigenic structure of the HIV gp120 envelope glycoprotein. Nature. 1998 Jun 18;393(6686):705–11.

12. Barouch DH. Challenges in the development of an HIV-1 vaccine. Nature. 2008 Oct 2;455(7213):613–9.

13. Plotkin SA. Increasing Complexity of Vaccine Development. J Infect Dis. 2015 Jul 15;212 Suppl 1:S12-16.

14. Wang HB, Mo QH, Yang Z. HIV vaccine research: the challenge and the way forward. J Immunol Res. 2015;2015:503978.

15. Miedema F. A brief history of HIV vaccine research: stepping back to the drawing board? AIDS Lond Engl. 2008 Sep 12;22(14):1699–703.

16. Dolin R, Graham BS, Greenberg SB, Tacket CO, Belshe RB, Midthun K, et al. The safety and immunogenicity of a human immunodeficiency virus type 1 (HIV-1) recombinant gp160 candidate vaccine in humans. NIAID AIDS Vaccine Clinical Trials Network. Ann Intern Med. 1991 Jan 15;114(2):119–27.

17. Cooney EL, Collier AC, Greenberg PD, Coombs RW, Zarling J, Arditti DE, et al. Safety of and immunological response to a recombinant vaccinia virus vaccine expressing HIV envelope glycoprotein. Lancet Lond Engl. 1991 Mar 9;337(8741):567–72.

18. Flynn NM, Forthal DN, Harro CD, Judson FN, Mayer KH, Para MF, et al. Placebo-controlled phase 3 trial of a recombinant glycoprotein 120 vaccine to prevent HIV-1 infection. J Infect Dis. 2005 Mar 1;191(5):654–65.

19. Pitisuttithum P, Gilbert P, Gurwith M, Heyward W, Martin M, van Griensven F, et al. Randomized, double-blind, placebo-controlled efficacy trial of a bivalent recombinant glycoprotein 120 HIV-1 vaccine among injection drug users in Bangkok, Thailand. J Infect Dis. 2006 Dec 15;194(12):1661–71.

20. McEnery R. HVTN 505 trial expanded to see if vaccine candidates can block HIV acquisition. IAVI Rep Newsl Int AIDS Vaccine Res. 2011;15(4):17.

21. Rerks-Ngarm S, Pitisuttithum P, Nitayaphan S, Kaewkungwal J, Chiu J, Paris R, et al. Vaccination with ALVAC and AIDSVAX to Prevent HIV-1 Infection in Thailand. N Engl J Med. 2009 Dec 3;361(23):2209–20.

22. Shubin Z, Stanfield-Oakley S, Puangkaew J, Pitisutthithum P, Nitayaphan S, Gurunathan S, et al. Additional boosting to the RV144 vaccine regimen increased Fc-mediated effector function magnitude but not durability. AIDS Lond Engl. 2023 Aug 1;37(10):1519–24.

23. Haynes BF, Gilbert PB, McElrath MJ, Zolla-Pazner S, Tomaras GD, Alam SM, et al. Immune-Correlates Analysis of an HIV-1 Vaccine Efficacy Trial. N Engl J Med. 2012 Apr 5;366(14):1275–86.

24. Chung AW, Ghebremichael M, Robinson H, Brown E, Choi I, Lane S, et al. Polyfunctional Fc-effector profiles mediated by IgG subclass selection distinguish RV144 and VAX003 vaccines. Sci Transl Med. 2014 Mar 19;6(228):228ra38.

25. Bf H, Pb G, Mj M, S ZP, Gd T, Sm A, et al. Immune-correlates analysis of an HIV-1 vaccine efficacy trial. N Engl J Med [Internet]. 2012 Apr 5 [cited 2024 Mar 17];366(14). Available from: https://pubmed.ncbi.nlm.nih.gov/22475592/

26. Gray GE, Huang Y, Grunenberg N, Laher F, Roux S, Andersen-Nissen E, et al. Immune correlates of the Thai RV144 HIV vaccine regimen in South Africa. Sci Transl Med. 2019 Sep 18;11(510):eaax1880.

27. Gray GE, Huang Y, Grunenberg N, Laher F, Roux S, Andersen-Nissen E, et al. Immune correlates of the Thai RV144 HIV vaccine regimen in South Africa. Sci Transl Med. 2019 Sep 18;11(510):eaax1880.

28. Bekker LG, Moodie Z, Grunenberg N, Laher F, Tomaras GD, Cohen KW, et al. Subtype C ALVAC-HIV and bivalent subtype C gp120/MF59 HIV-1 vaccine in low-risk, HIV-uninfected, South African adults: a phase 1/2 trial. Lancet HIV. 2018 Jul;5(7):e366–78.

29. Cohen J. Combo of two HIV vaccines fails its big test. Science. 2020 Feb 7;367(6478):611–2.

30. Caniels TG, Medina-Ramírez M, Zhang J, Sarkar A, Kumar S, LaBranche A, et al. Germline-targeting HIV-1 Env vaccination induces VRC01-class antibodies with rare insertions. Cell Rep Med. 2023 Apr 18;4(4):101003.

31. Leggat DJ, Cohen KW, Willis JR, Fulp WJ, deCamp AC, Kalyuzhniy O, et al. Vaccination induces HIV broadly neutralizing antibody precursors in humans. Science. 2022 Dec 2;378(6623):eadd6502.

32. Corey L, Gilbert PB, Juraska M, Montefiori DC, Morris L, Karuna ST, et al. Two Randomized Trials of Neutralizing Antibodies to Prevent HIV-1 Acquisition. N Engl J Med. 2021 Mar 18;384(11):1003–14.

33. Human Immunodeficiency Virus (HIV). Transfus Med Hemotherapy. 2016 May;43(3):203–22.

34. Cenker JJ, Stultz RD, McDonald D. Brain Microglial Cells Are Highly Susceptible to HIV-1 Infection and Spread. AIDS Res Hum Retroviruses. 2017 Nov 1;33(11):1155–65.

35. Leonard CK, Spellman MW, Riddle L, Harris RJ, Thomas JN, Gregory TJ. Assignment of intrachain disulfide bonds and characterization of potential glycosylation sites of the type 1 recombinant human immunodeficiency virus envelope glycoprotein (gp120) expressed in Chinese hamster ovary cells. J Biol Chem. 1990 Jun 25;265(18):10373–82.

36. Christensen DE, Ganser-Pornillos BK, Johnson JS, Pornillos O, Sundquist WI. Reconstitution and visualization of HIV-1 capsid-dependent replication and integration in vitro. Science. 2020 Oct 9;370(6513):eabc8420.

37. Li Z, Li W, Lu M, Bess J, Chao CW, Gorman J, et al. Subnanometer structures of HIV-1 envelope trimers on aldrithiol-2-inactivated virus particles. Nat Struct Mol Biol. 2020 Aug;27(8):726–34.

38. Lu M, Ma X, Castillo-Menendez LR, Gorman J, Alsahafi N, Ermel U, et al. Associating HIV-1 envelope glycoprotein structures with states on the virus observed by smFRET. Nature. 2019 Apr;568(7752):415–9.

39. Munro JB, Gorman J, Ma X, Zhou Z, Arthos J, Burton DR, et al. Conformational dynamics of single HIV-1 envelope trimers on the surface of native virions. Science. 2014 Nov 7;346(6210):759–63.

40. Stadtmueller BM, Bridges MD, Dam KM, Lerch MT, Huey-Tubman KE, Hubbell WL, et al. DEER Spectroscopy Measurements Reveal Multiple Conformations of HIV-1 SOSIP Envelopes that Show Similarities with Envelopes on Native Virions. Immunity. 2018 Aug 21;49(2):235-246.e4.

41. Alsahafi N, Bakouche N, Kazemi M, Richard J, Ding S, Bhattacharyya S, et al. An Asymmetric Opening of HIV-1 Envelope Mediates Antibody-Dependent Cellular Cytotoxicity. Cell Host Microbe. 2019 Apr 10;25(4):578-587.e5.

42. Jette CA, Barnes CO, Kirk SM, Melillo B, Smith AB, Bjorkman PJ. Cryo-EM structures of HIV-1 trimer bound to CD4-mimetics BNM-III-170 and M48U1 adopt a CD4-bound open conformation. Nat Commun. 2021 Mar 29;12(1):1950.

43. Yang Z, Wang H, Liu AZ, Gristick HB, Bjorkman PJ. Asymmetric opening of HIV-1 Env bound to CD4 and a coreceptor-mimicking antibody. Nat Struct Mol Biol. 2019 Dec;26(12):1167–75.

44. Stanfield RL, Wilson IA. Antibody Structure. Microbiol Spectr. 2014 Mar 21;2(2):2.2.06.

45. Richardson SI, Lambson BE, Crowley AR, Bashirova A, Scheepers C, Garrett N, et al. IgG3 enhances neutralization potency and Fc effector function of an HIV V2-specific broadly neutralizing antibody. Doores KJ, editor. PLOS Pathog. 2019 Dec 16;15(12):e1008064.

46. Chu TH, Crowley AR, Backes I, Chang C, Tay M, Broge T, et al. Hinge length contributes to the phagocytic activity of HIV-specific IgG1 and IgG3 antibodies. Doores KJ, editor. PLOS Pathog. 2020 Feb 24;16(2):e1008083.

47. Antibody Structure & Isotypes - Creative Biolabs [Internet]. [cited 2022 Nov 25]. Available from: https://www.antibody-creativebiolabs.com/antibody-structure-isotypes.htm

48. Normansell DE. Human immunoglobulin subclasses. Diagn Clin Immunol. 1987;5(3):115–28.

49. Torres M, Casadevall A. The immunoglobulin constant region contributes to affinity and specificity. Trends Immunol. 2008 Feb;29(2):91–7.

50. Gray ES, Moody MA, Wibmer CK, Chen X, Marshall D, Amos J, et al. Isolation of a Monoclonal Antibody That Targets the Alpha-2 Helix of gp120 and Represents the Initial Autologous Neutralizing-Antibody Response in an HIV-1 Subtype C-Infected Individual ▿. J Virol. 2011 Aug;85(15):7719–29.

51. Doria-Rose NA, Klein RM, Daniels MG, O'Dell S, Nason M, Lapedes A, et al. Breadth of human immunodeficiency virus-specific neutralizing activity in sera: clustering analysis and association with clinical variables. J Virol. 2010 Feb;84(3):1631–6.

52. Moore PL, Gray ES, Sheward D, Madiga M, Ranchobe N, Lai Z, et al. Potent and broad neutralization of HIV-1 subtype C by plasma antibodies targeting a quaternary epitope including residues in the V2 loop. J Virol. 2011 Apr;85(7):3128–41.

53. Hraber P, Seaman MS, Bailer RT, Mascola JR, Montefiori DC, Korber BT. Prevalence of broadly neutralizing antibody responses during chronic HIV-1 infection. AIDS Lond Engl. 2014 Jan 14;28(2):163–9.

54. Parker Miller E, Finkelstein MT, Erdman MC, Seth PC, Fera D. A Structural Update of Neutralizing Epitopes on the HIV Envelope, a Moving Target. Viruses. 2021 Sep 5;13(9):1774.

55. Kwong PD, Mascola JR. HIV-1 Vaccines Based on Antibody Identification, B Cell Ontogeny, and Epitope Structure. Immunity. 2018 May 15;48(5):855–71.

56. Chuang GY, Zhou J, Rawi R, Shen CH, Sheng Z, West AP, et al. Structural survey of HIV-1-neutralizing antibodies targeting Env trimer delineates epitope categories and suggests vaccine templates [Internet]. bioRxiv; 2018 [cited 2023 May 7]. p. 312579. Available from: https://www.biorxiv.org/content/10.1101/312579v1

57. Parsons MS, Chung AW, Kent SJ. Importance of Fc-mediated functions of anti-HIV-1 broadly neutralizing antibodies. Retrovirology. 2018 Dec;15(1):58.

58. MBBS AA, PhD ALM, PhD SPM. Cellular and Molecular Immunology: with STUDENT CONSULT Online Access. 7th edition. Philadelphia: Saunders; 2011. 560 p.

59. M T, C G, S J, M M, D M, C L, et al. Improved killing of HIV-infected cells using three neutralizing and non-neutralizing antibodies. J Clin Invest [Internet]. 2020 Oct 1 [cited 2024 Mar 17];130(10). Available from: https://pubmed.ncbi.nlm.nih.gov/32584790/

60. Richardson SI, Chung AW, Natarajan H, Mabvakure B, Mkhize NN, Garrett N, et al. HIV-specific Fc effector function early in infection predicts the development of broadly neutralizing antibodies. PLoS Pathog. 2018 Apr 9;14(4):e1006987.

61. Richardson SI, Crowther C, Mkhize NN, Morris L. Measuring the ability of HIV-specific antibodies to mediate trogocytosis. J Immunol Methods. 2018 Dec;463:71–83.

62. Lin LY, Carapito R, Su B, Moog C. Fc receptors and the diversity of antibody responses to HIV infection and vaccination. Genes Immun. 2022 Aug;23(5):149–56.

63. Daëron M. Fc receptor biology. Annu Rev Immunol. 1997;15:203–34.

64. Reth M. Antigen receptor tail clue. Nature. 1989 Mar 30;338(6214):383–4.

65. Su K, Wu J, Edberg JC, McKenzie SE, Kimberly RP. Genomic organization of classical human low-affinity Fcgamma receptor genes. Genes Immun. 2002 Oct;3 Suppl 1:S51-56.

66. Bruhns P, Iannascoli B, England P, Mancardi DA, Fernandez N, Jorieux S, et al. Specificity and affinity of human Fcγ receptors and their polymorphic variants for human IgG subclasses. Blood. 2009 Apr 16;113(16):3716–25.

67. Alemán OR, Mora N, Rosales C. The Antibody Receptor Fc Gamma Receptor IIIb Induces Calcium Entry via Transient Receptor Potential Melastatin 2 in Human Neutrophils. Front Immunol. 2021;12:657393.

68. Bohannon C, Powers R, Satyabhama L, Cui A, Tipton C, Michaeli M, et al. Long-lived antigen-induced IgM plasma cells demonstrate somatic mutations and contribute to long-term protection. Nat Commun. 2016 Jun 7;7:11826.

69. Sterlin D, Fadlallah J, Adams O, Fieschi C, Parizot C, Dorgham K, et al. Human IgA binds a diverse array of commensal bacteria. J Exp Med. 2020 Mar 2;217(3):e20181635.

70. Stapleton NM, Andersen JT, Stemerding AM, Bjarnarson SP, Verheul RC, Gerritsen J, et al. Competition for FcRn-mediated transport gives rise to short half-life of human IgG3 and offers therapeutic potential. Nat Commun. 2011 Sep;2(1):599.

71. van der Zee JS, van Swieten P, Aalberse RC. Serologic aspects of IgG4 antibodies. II. IgG4 antibodies form small, nonprecipitating immune complexes due to functional monovalency. J Immunol Baltim Md 1950. 1986 Dec 1;137(11):3566–71.

72. Bruhns P, Iannascoli B, England P, Mancardi DA, Fernandez N, Jorieux S, et al. Specificity and affinity of human Fcgamma receptors and their polymorphic variants for human IgG subclasses. Blood. 2009 Apr 16;113(16):3716–25.

73. James LK. B cells defined by immunoglobulin isotypes. Clin Exp Immunol. 2022 Dec 31;210(3):230–9.

74. Nm V, Mj H, Ef R. Antibody Subclass Repertoire and Graft Outcome Following Solid Organ Transplantation. Front Immunol [Internet]. 2016 Oct 24 [cited 2023 Jul 3];7. Available from: https://pubmed.ncbi.nlm.nih.gov/27822209/

75. The Immunoglobulin Factsbook by Lefranc, M.-P. and Lefranc, G.: Good (2001) | Anybook Ltd. [Internet]. [cited 2023 Apr 13]. Available from: https://www.abebooks.com/9780124413511/Immunoglobulin-Factsbook-Lefranc-M.-P-G-012441351X/plp

76. Vidarsson G, Dekkers G, Rispens T. IgG Subclasses and Allotypes: From Structure to Effector Functions. Front Immunol [Internet]. 2014 [cited 2023 Apr 12];5. Available from: https://www.frontiersin.org/articles/10.3389/fimmu.2014.00520

77. Bashirova AA, Zheng W, Akdag M, Augusto DG, Vince N, Dong KL, et al. Population-specific diversity of the immunoglobulin constant heavy G chain (IGHG) genes. Genes Immun. 2021 Dec;22(7):327–34.

78. Lefranc MP. IMGT, the international ImMunoGeneTics database. Nucleic Acids Res. 2001 Jan 1;29(1):207–9.

79. de Taeye SW, Rispens T, Vidarsson G. The Ligands for Human IgG and Their Effector Functions. Antibodies. 2019 Jun;8(2):30.

80. Lu Y, Harding SE, Michaelsen TE, Longman E, Davis KG, Ortega A, et al. Solution conformation of wild-type and mutant IgG3 and IgG4 immunoglobulins using crystallohydrodynamics: possible implications for complement activation. Biophys J. 2007 Dec 1;93(11):3733–44.

81. Dugast AS, Tonelli A, Berger CT, Ackerman ME, Sciaranghella G, Liu Q, et al. Decreased Fc-Receptor expression on innate immune cells is associated with impaired antibody mediated cellular phagocytic activity in chronically HIV-1 infected individuals. Virology. 2011 Jul 5;415(2):160–7.

82. Lefranc MP, Lefranc G. Human Gm, Km, and Am allotypes and their molecular characterization: a remarkable demonstration of polymorphism. Methods Mol Biol Clifton NJ. 2012;882:635–80.

83. Richardson SI, Ayres F, Manamela NP, Oosthuysen B, Makhado Z, Lambson BE, et al. HIV Broadly Neutralizing Antibodies Expressed as IgG3 Preserve Neutralization Potency and Show Improved Fc Effector Function. Front Immunol. 2021 Sep 10;12:733958.

84. Lefranc MP, Lefranc G. Human Gm, Km, and Am allotypes and their molecular characterization: a remarkable demonstration of polymorphism. Methods Mol Biol Clifton NJ. 2012;882:635–80.

85. Jefferis R, Lefranc MP. Human immunoglobulin allotypes. mAbs. 2009 Aug 1; 1(4):332–8.

86. Ak W, W K. Beyond Allotypes: The Influence of Allelic Diversity in Antibody Constant Domains. Front Immunol [Internet]. 2020 Aug 18 [cited 2024 Mar 17];11. Available from: https://pubmed.ncbi.nlm.nih.gov/32973808/

87. Warrender AK, Kelton W. Beyond Allotypes: The Influence of Allelic Diversity in Antibody Constant Domains. Front Immunol. 2020;11:2016.

88. de Taeye SW, Bentlage AEH, Mebius MM, Meesters JI, Lissenberg-Thunnissen S, Falck D, et al. FcγR Binding and ADCC Activity of Human IgG Allotypes. Front Immunol. 2020 May 6;11:740.

89. van Loggerenberg F, Mlisana K, Williamson C, Auld SC, Morris L, Gray CM, et al. Establishing a Cohort at High Risk of HIV Infection in South Africa: Challenges and Experiences of the CAPRISA 002 Acute Infection Study. PLoS ONE. 2008 Apr 16;3(4):e1954.

90. Doria-Rose NA, Bhiman JN, Roark RS, Schramm CA, Gorman J, Chuang GY, et al. New Member of the V1V2-Directed CAP256-VRC26 Lineage That Shows Increased Breadth and Exceptional Potency. Silvestri G, editor. J Virol. 2016 Jan;90(1):76–91.

91. Sok D, Burton DR. Recent progress in broadly neutralizing antibodies to HIV. Nat Immunol. 2018 Nov;19(11):1179–88.

92. Gorman J, Chuang GY, Lai YT, Shen CH, Boyington JC, Druz A, et al. Structure of Super-Potent Antibody CAP256-VRC26.25 in Complex with HIV-1 Envelope Reveals a Combined Mode of Trimer-Apex Recognition. Cell Rep. 2020 Apr 7;31(1):107488.

93. Mahomed S, Garrett N, Karim QA, Zuma NY, Capparelli E, Baxter C, et al. Assessing the safety and pharmacokinetics of the anti-HIV monoclonal antibody CAP256V2LS alone and in combination with VRC07-523LS and PGT121 in South African women: study protocol for the first-in-human CAPRISA 012B phase I clinical trial. BMJ Open. 2020 Nov 1;10(11):e042247.

94. Mahomed S, Garrett N, Capparelli EV, Osman F, Mkhize NN, Harkoo I, et al. Safety and pharmacokinetics of escalating doses of neutralising monoclonal antibody CAP256V2LS administered with and without VRC07-523LS in HIV-negative women in South Africa (CAPRISA 012B): a phase 1, dose-escalation, randomised controlled trial. Lancet HIV. 2023 Apr;10(4):e230–43.

95. Karim SA. CAPRISA 002 Viral set point and clinical disease progression: The role of immunological, genetic and viral factors over the course of disease and during antiretroviral therapy [Internet]. 2017 [cited 2023 Sep 14]. Available from: https://www.caprisa.org

96. Spencer H. Functional impact of IGHG3 genetic variation in HIV-1 infection [Master`s Dissertation]. [Johannesburg]: University of the Witwatersrand; 2021.

97. Edelman GM, Cunningham BA, Gall WE, Gottlieb PD, Rutishauser U, Waxdal MJ. THE COVALENT STRUCTURE OF AN ENTIRE γG IMMUNOGLOBULIN MOLECULE*. Proc Natl Acad Sci U S A. 1969 May;63(1):78–85.

98. Zhang Y, Wang Y, Li Y. Major cause of antibody artifact bands on non-reducing SDS-PAGE and methods for minimizing artifacts. Protein Expr Purif. 2019 Dec;164:105459.

99. Moyo-Gwete T, Scheepers C, Makhado Z, Kgagudi P, Mzindle NB, Ziki R, et al. Enhanced neutralization potency of an identical HIV neutralizing antibody expressed as different isotypes is achieved through genetically distinct mechanisms. Sci Rep. 2022 Oct 1;12:16473.

100. Scheepers C, Bekker V, Anthony C, Richardson SI, Oosthuysen B, Moyo T, et al. Antibody Isotype Switching as a Mechanism to Counter HIV Neutralization Escape. Cell Rep. 2020 Nov;33(8):108430.

101. Crowley AR, Richardson SI, Tuyishime M, Jennewein M, Bailey MJ, Lee J, et al. Functional consequences of allotypic polymorphisms in human immunoglobulin G subclasses. Immunogenetics. 2023 Feb;75(1):1–16.

102. Natsume A, In M, Takamura H, Nakagawa T, Shimizu Y, Kitajima K, et al. Engineered antibodies of IgG1/IgG3 mixed isotype with enhanced cytotoxic activities. Cancer Res. 2008 May 15;68(10):3863–72.

103. Rispens T, Davies AM, Ooijevaar-de Heer P, Absalah S, Bende O, Sutton BJ, et al. Dynamics of inter-heavy chain interactions in human immunoglobulin G (IgG)

subclasses studied by kinetic Fab arm exchange. J Biol Chem. 2014 Feb 28;289(9):6098–109.

Appendix A: Human Research Ethics Committee (HREC) Approval of parent project

UNIVERSITY OF THE WITWATERSRAND, JOHANNESBURG	HUMAN RESEARCH ETHICS COMMITTEE (MEDICAL)

2022/11/11

Professor P Moore, et al
Centre for HIV & Sexually Transmitted Infections
National Institute for Communicable Diseases
1 Modderfontein Road
Sandringham
2031

Sent by e-mail to: carolc@nicd.ac.za

Dear Dr Crowther

Re: **Protocol Ref No:** M210892
Protocol Title: *Viral set point and clinical disease progression: The role of immunological, genetic and viral factors over the course of disease and during antiretroviral therapy*
Principal Investigators: Professor P Moore, et al

Thank you for your letter of 2022/11/07.

We note and approve of your progress report and the impressive list of publications. As such, your current ethics clearance remains valid until 2026/09/06, subject to continued satisfactory progress.

Thank you for keeping us informed.

Yours Sincerely

.....
Mr I Burns
For the Human Research Ethics Committee (Medical)

.....
Dr N Naran, Co-Chairperson, Human Research Ethics Committee (Medical)

Appendix B: Human Research Ethics Committee (HREC) Waiver letter

UNIVERSITY OF THE WITWATERSRAND JOHANNESBURG

R49 Mr OK Fonguh

HUMAN RESEARCH ETHICS COMMITTEE (MEDICAL)
CLEARANCE CERTIFICATE NO. M2211125

NAME: (Principal Investigator)	Mr OK Fonguh
DEPARTMENT:	School of Pathology Department of Chemical Pathology Medical School University
PROJECT TITLE:	*Functional consequences of novel IgG3 allelic variation CAP256-VRC26.25*
DATE CONSIDERED:	Ad hoc
DECISION:	Approved unconditionally
CONDITIONS:	Sub-study under M21/08/92
NOTE:	If contact information regarding student study participants is required, please contact the Registrar's office - <Nicoleen.Potgieter@wits.ac.za>
SUPERVISOR:	Dr S Richardson and Professor P Moore
APPROVED BY:	Dr N Naran, Co-Chairperson, HREC (Medical)
DATE OF APPROVAL:	2023/01/09

This Clearance Certificate is valid for 5 years from the date of approval. An extension may be applied for.

DECLARATION OF INVESTIGATORS

To be completed in duplicate and **ONE COPY** returned to the Research Office secretariat on the 3rd floor, Phillip Tobias Building, Parktown, University of the Witwatersrand, Johannesburg.

I/we fully understand the conditions under which I am/we are authorized to carry out the above-mentioned research and I/we undertake to ensure compliance with these conditions. Should any departure be contemplated from the research protocol as approved, I/we undertake to submit details to the Committee. **I agree to submit a yearly progress report**. When a funder requires annual re-certification, the application date will be one year after the date when the study was initially reviewed. In this case, the study was initially reviewed in **November** and therefore reports and re-certification will be due in the month of **November** each year. Unreported changes to the study may invalidate the clearance given by the HREC (Medical).

Signature of Principal Investigator — Date: 2023/01/11

Appendix C: Plagiarism declaration

PLAGIARISM DECLARATION TO BE SIGNED BY ALL HIGHER DEGREE STUDENTS

SENATE PLAGIARISM POLICY: APPENDIX ONE

I Fonguh Oliver Khan (Student number: 2626981) am a student registered for the

degree of Master in Vaccinology in the academic year 2023.

I hereby declare the following:

- I am aware that plagiarism (the use of someone else's work without their permission and/or without acknowledging the original source) is wrong.
- I confirm that the work submitted for assessment for the above degree is my own unaided work except where I have explicitly indicated otherwise.
- I have followed the required conventions in referencing the thoughts and ideas of others.
- I understand that the University of the Witwatersrand may take disciplinary action against me if there is a belief that this is not my own unaided work or that I have failed to acknowledge the source of the ideas or words in my writing.
- I have included as an appendix a report from "Turnitin" (or other approved plagiarism detection) software indicating the level of plagiarism in my research document.

Signature: _____ Date: 6th December 2023

Appendix D: Turnitin Report

2626981_Oliver K Fonguh_Reseach Report Turnitin.docx

ORIGINALITY REPORT

17%	11%	9%	9%
SIMILARITY INDEX	INTERNET SOURCES	PUBLICATIONS	STUDENT PAPERS

PRIMARY SOURCES

1	Submitted to University of Witwatersrand Student Paper	4%
2	www.ncbi.nlm.nih.gov Internet Source	1%
3	Simone I. Richardson, Bronwen E. Lambson, Andrew R. Crowley, Arman Bashirova et al. "IgG3 enhances neutralization potency and Fc effector function of an HIV V2-specific broadly neutralizing antibody", PLOS Pathogens, 2019 Publication	1%
4	eprints.nottingham.ac.uk Internet Source	<1%
5	patents.google.com Internet Source	<1%
6	etheses.bham.ac.uk Internet Source	<1%
7	www.mdpi.com Internet Source	<1%
8	mediatum.ub.tum.de Internet Source	